Table 1 | EC_{50} of vitamin A compounds on HCV RNA replication

	Peretinoin		ATRA		9-cis RA		13-cis RA	
	Mean	SD	Mean	SD	Mean	SD	Mean	SD
HCV	(μM)	(μM)	(μM)	(μM)	(μM)	(μM)	(μM)	(μM)
H77S.3	9	1	32	3	29	7	41	4
N.2	19	1	53	5	75	8	83	17
HJ3-5	18	2	25	1	51	6	82	17
JFH1	20	1	25	1	61	8	78	11

impact of Peretinoin on lipid metabolism by measuring intracellular triglyceride (TG) levels, which should mainly reflect the amount of LDs, following treatment with 0–40 μM Peretinoin with or without HCV replication and OA treatment. Peretinoin reduced intracellular TG levels in a dose-dependent manner, regardless of OA treatment and HCV replication (Fig. 4A). These effects may be primarily due to its transcriptional modulation. To address this possibility, we examined the effect of Peretinoin on the transcription of fatty acid synthase (FASN) using RTD-PCR under 0–40 μM Peretinoin with or without HCV replication and OA treatment, because FASN is a key enzyme for the synthesis of fatty acids, which are an essential component of TGs. Peretinoin reduced the mRNA levels of FASN in a dose-dependent manner, regardless of OA treatment and HCV replication (Fig. 4B). We also examined FASN protein expression as well as the levels of precursor and mature sterol regulatory element-binding protein 1c (SREBP1c), which is a critical transcription factor for FASN. Peretinoin reduced the expression of FASN protein, which is consistent with the RTD-PCR results (Fig. 4C, see Supplementary Fig. S7 online). Although Peretinoin did not have an effect on precursor SREBP1c protein expression, it dramatically reduced the levels of mature SREBP1c (Fig. 4C, see Supplementary Fig. S7 online). We also observed a reduction of FASN mRNA levels by Peretinoin in an immortalised human hepatocyte cell line (Fig. 5A), and a similar reduction was also observed for ATRA, 9-cis RA, and 13-cis RA treatment of HCV-replicating Huh-7.5 cells (Fig. 5B). These results indicate that Peretinoin reduced intracellular lipid levels by reducing the amount of mature SREBP1c and, subsequently, FASN.

Specific inhibition of virus secretion by Peretinoin. Recently, lipids including LDs and TG have been reported to be important for efficient infectious virus production[14–16]. Due to its huge impact on lipid metabolism, Peretinoin could affect virus assembly or secretion as well as RNA amplification. To test the effect of Peretinoin on infectious virus production, we determined intra- and extra-cellular infectivity and the virus secretion ratio by measuring the amount of intra- and extra-cellular infectious virus from HJ3-5/GLuc2A-replicating FT3-7 cells treated with various concentrations of Peretinoin. We infected naïve Huh-7.5 cells with intra- and extra-cellular virus derived from HJ3-5/GLuc2A-replicating cells after Peretinoin treatment and used GLuc activity as an indicator of infectious virus production because FFUs and GLuc activity were well correlated (see Supplementary Fig. S8 online),

Table 2 | CC_{50} of vitamin A compounds on Huh-7.5 cells supporting HCV replication

Peretinoin		ATRA	9-cis RA	13-cis RA
Mean	SD	Mean	Mean	Mean
(μM)	(μM)	(μM)	(μM)	(μM)
68	5.2	>100	>100	>100

and a previous report also showed a good correlation between them[17]. Although Peretinoin did not show a significant impact on intracellular infectivity at 10–30 μM, it dramatically reduced extracellular infectivity and virus secretion from 10 μM when we normalised intra- and extra-cellular infectivity by the replication capacity of the virus producing the intra- and extra-cellular virus, as determined by GLuc activity (Fig. 6A). This result was also confirmed by using the extra-cellular virus which was prepared by centrifugation and subsequently re-suspended to fresh medium without containing Peretinoin, indicating that possible carryover of Peretinoin in the medium from extra-cellular cultures does not affect the result shown in Figure 6A (Supplementary Fig. S9 online). Interestingly, the expression of apolipoprotein E3 (ApoE3), which is essential for virus secretion, was also suppressed by Peretinoin (Fig. 4C, see Supplementary Fig. S7 online). Furthermore, we compared the buoyant density of HCVcc derived from HJ3-5/GLuc2A-replicating FT3-7 cells by equilibrium gradient ultracentrifugation. HCVcc from HJ3-5/GLuc2A-replicating cells treated with dimethyl sulfoxide (DMSO) or 30 μM Peretinoin showed exactly the same peak of infectivity at 1.107 g/cm^3 (Fig. 6B, 6C). Specific infectivity, as calculated from both peaks of HCV RNA and GLuc activity, was 0.0381 ± 0.0209 (standard deviation, SD) light units (LU)/copy for DMSO-treated cells, and 0.0799 ± 0.0457 LU/copy for Peretinoin-treated cells, which did not show a considerable difference. Furthermore, Peretinoin did not affect virus entry of HCVcc when we tested it by RT-PCR for HCV RNA at 5 h after infection and an FFU assay at 72 h after infection (see Supplementary Fig. S10 online). Collectively, Peretinoin seems to inhibit virus release in addition to viral RNA amplification.

Discussion

In the present study, we clearly showed that Peretinoin, as well as ATRA, 9-cis RA, and 13-cis RA, suppressed HCV RNA replication (Table 1). While previous reports used replicon systems to test the effects of retinoids, we used a genome-length HCV containing a GLuc-coding sequence between p7 and NS2, which is more physiological than replicons. The inhibitory effect of retinoids was universal among the HCV genotypes tested, and all retinoids tested showed an inhibitory effect on HCV replication (Table 1). In addition, we also observed the antiviral effect of Peretinoin in the replicon system (Fig. 1E). Therefore, our present data strongly support the notion that retinoids exert an antiviral effect *in vitro*. The antiviral effect of retinoids has also been confirmed in a clinical study. Even when CH-C patients were treated with ATRA, the viral load dropped by 1–2 log units in 50% of the patients enrolled. In addition, when CH-C patients who showed no response to prior IFN/PEG-IFNα and ribavirin therapy were treated with a combination of ATRA and PEG-IFNα-2a, 30% of patients showed a significant viral reduction[18]. Recently, combined vitamin A and D deficiency prior to IFN-based therapy was shown to be a strong independent predictor of non-response to antiviral therapy[19]. Collectively, our data and the clinical findings indicate that retinoids possess inhibitory effects on HCV replication.

Peretinoin showed the strongest antiviral effect among the retinoids tested (Table 1); thus, we focused on Peretinoin to clarify its antiviral mechanism. A previous report showed that 9-cis RA enhanced the antiviral effect of IFNα by increasing the expression of the IFNα receptor[20]; however, another study showed that ATRA did not induce the activation of dsRNA-activated protein kinase R, which is a key player in the IFN-induced antiviral response[7]. In the present study, Peretinoin did not increase the amount of the activated form of STAT-1, which is pSTAT1, contrary to IFNα-2b, both in HCV-replicating and HCV-non replicating Huh-7.5 cells, and dual treatment of Huh-7.5 cells with IFNα-2b and Peretinoin did not show a further increase of the pSTAT1 levels induced by only IFNα-2b (see Supplementary Fig. S4 online), indicating that

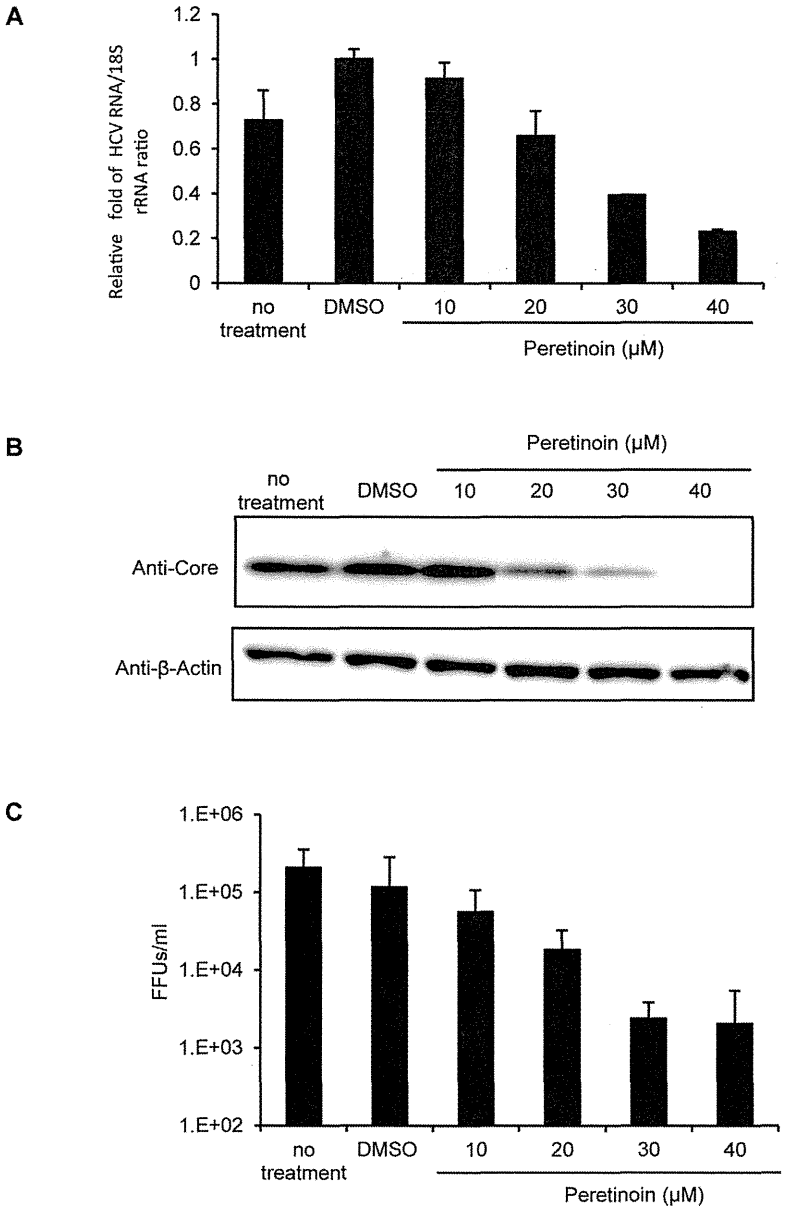

Figure 2 | Inhibition of HCV replication and infectious virus production. Huh-7.5 cells were infected with the HJ3-5 virus at a multiplicity of infection (MOI) of 1, and 72 h later, DMSO or Peretinoin was added at the indicated concentrations. The medium was replaced with fresh medium every 24 h until 72 h. (A) At 72 h after adding Peretinoin, total cellular RNA was extracted, and the amount of HCV RNA and 18S rRNA was quantitated by RTD-PCR. Relative HCV RNA abundance normalised to the amount of 18S rRNA is presented as fold change ± SD compared to DMSO-treated cells from 3 independent experiments. (B) At 72 h after Peretinoin treatment, the cell lysates were collected and subjected to western blot analysis using anti-core protein and anti-β-actin antibodies. Full-length blots/gels are presented in Supplementary Fig. S2 online. (C) The medium was collected at 72 h after Peretinoin treatment, and immediately, naïve Huh-7.5 cells were infected with serially diluted medium. At 72 h after infection, the infectious virus titre of HCVcc from Peretinoin-treated cells was determined by an FFU assay. Data shown here represent the mean FFUs/mL ± SD from 2 independent experiments.

Peretinoin did not activate or enhance cellular IFN signalling. Our results also indicate that the antiviral effect of Peretinoin is not due to the suppression of HCV translation directed by HCV IRES (see Supplementary Fig. S3 online). As Peretinoin suppressed the RNA replication of bicistronic sub-genomic replicons (Fig. 1E), it seems to suppress RNA amplification itself (see also the later description of FASN). A report showed that retinoids inhibited HCV RNA replication by enhancing the expression of gastrointestinal-glutathione peroxidase (GI-GPx) only in the presence of sodium selenite[7]; however, in the present study, we demonstrated that all retinoids tested inhibited HCV replication, even in the absence of sodium selenite. Thus, our results support the notion that the observed antiviral effects could be independent of GI-GPx, although supplementation with sodium selenite may further enhance the antiviral effects of retinoids.

To clarify the mechanism underlying the antiviral effect of Peretinoin further, we focused on the effect of Peretinoin on lipid metabolism because it has been shown to modify multiple aspects of HCV infection[14–16], and we detected a significant reduction of FASN

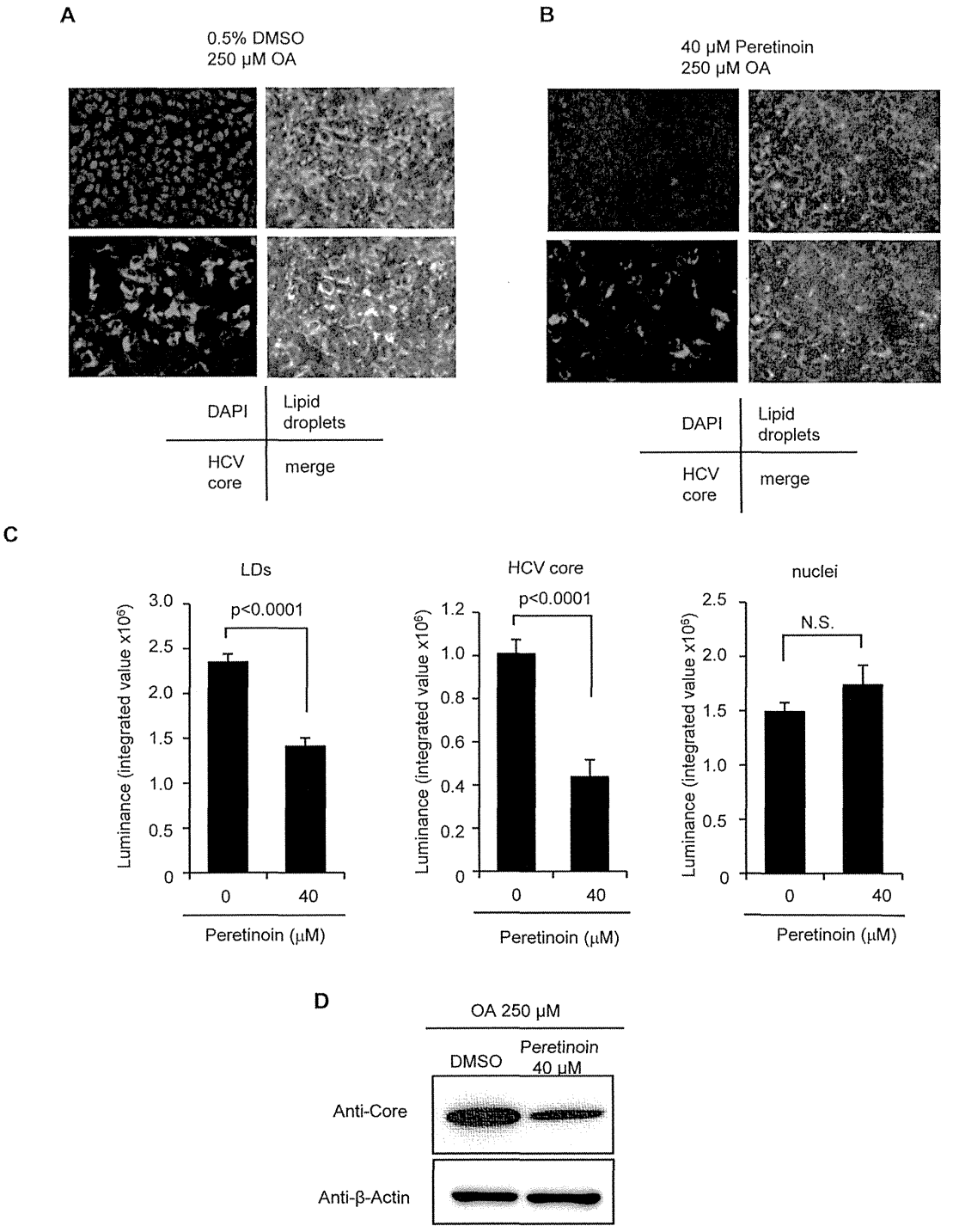

Figure 3 | Reduction of LD signals by Peretinoin. Huh-7.5 cells were infected with HJ3-5 virus at an MOI of 1, and 72 h later, 250 μM OA and DMSO or 250 μM OA and 40 μM Peretinoin were added, and the following assay was performed at 72 h later. (A, B) At 72 h later, the cells were fixed and stained for nuclei, LDs, and HCV core protein. (A) Shows 250 μM OA and DMSO-treated cells and (B) shows 250 μM OA and 40 μM Peretinoin-treated cells. The photos in (A) and (B) were taken under exactly the same conditions. (C) The signal intensity from LDs, HCV core protein, and nuclei was quantitated as described in the Methods. Data shown represent mean signal intensity ± SD from 4 different areas, and the difference was analysed statistically using Student's t-test. (D) Cell lysates were collected and subjected to western blot analysis using anti-core protein and anti-β-actin antibodies. Full-length blots/gels are presented in Supplementary Fig. S6 online. N.S., not significant.

mRNA levels by Peretinoin in a mouse hepatoma model, implying its possible effect on lipid metabolism[5]. Surprisingly, Peretinoin strongly reduced the signal from LDs in the presence of OA and intracellular TGs (Fig. 3A–C, 4A). LDs are known to have an essential role in the assembly of HCV virus particles by interacting with HCV core protein and NS5A[21,22]. Therefore, we examined the effect of Peretinoin on several steps of infectious virus production, such as assembly and secretion. Interestingly, Peretinoin specifically

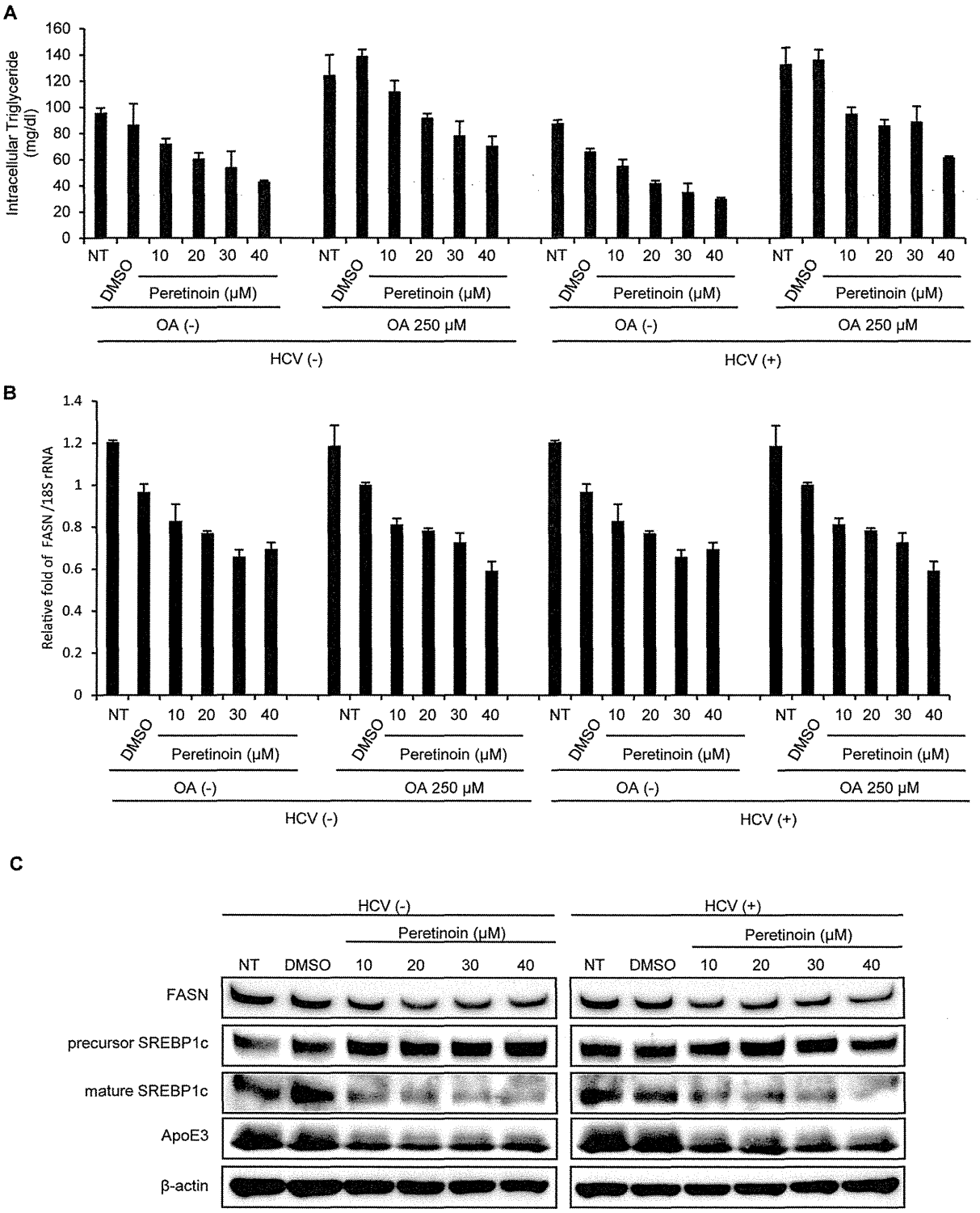

Figure 4 | Mechanism by which Peretinoin alters lipid metabolism. Huh-7.5 cells were transfected with H77S.3/GLuc2A RNA, and 72 h later, the transfected cells, depicted as 'HCV(+)', and non-transfected Huh-7.5 cells, depicted as 'HCV(-)', were treated with or without 250 μM OA in the presence of 2% fatty acid-free BSA with 0.5% DMSO or 10–40 μM Peretinoin, and the following assay was performed at 72 h later. (A) The concentration of intracellular TGs was measured. Data shown represent mean concentration ± SD from 3 independent experiments. (B) RNA was extracted and the levels of FASN mRNA and 18S rRNA were quantitated by RTD-PCR. FASN levels were normalised to those of 18S rRNA, and the ratio was furthermore normalised to that from DMSO-treated cells. The results presented here represent the relative fold of FASN/18S rRNA ± SD from 3 independent experiments at the indicated conditions. (C) Lysates from the cells without OA treatment were collected and subjected to western blot analysis using anti-FASN, anti-precursor SREBP1c, anti-mature SREBP1c, anti-ApoE3, and anti-β-actin antibodies. Full-length blots/gels are presented in Supplementary Fig. S7 online.

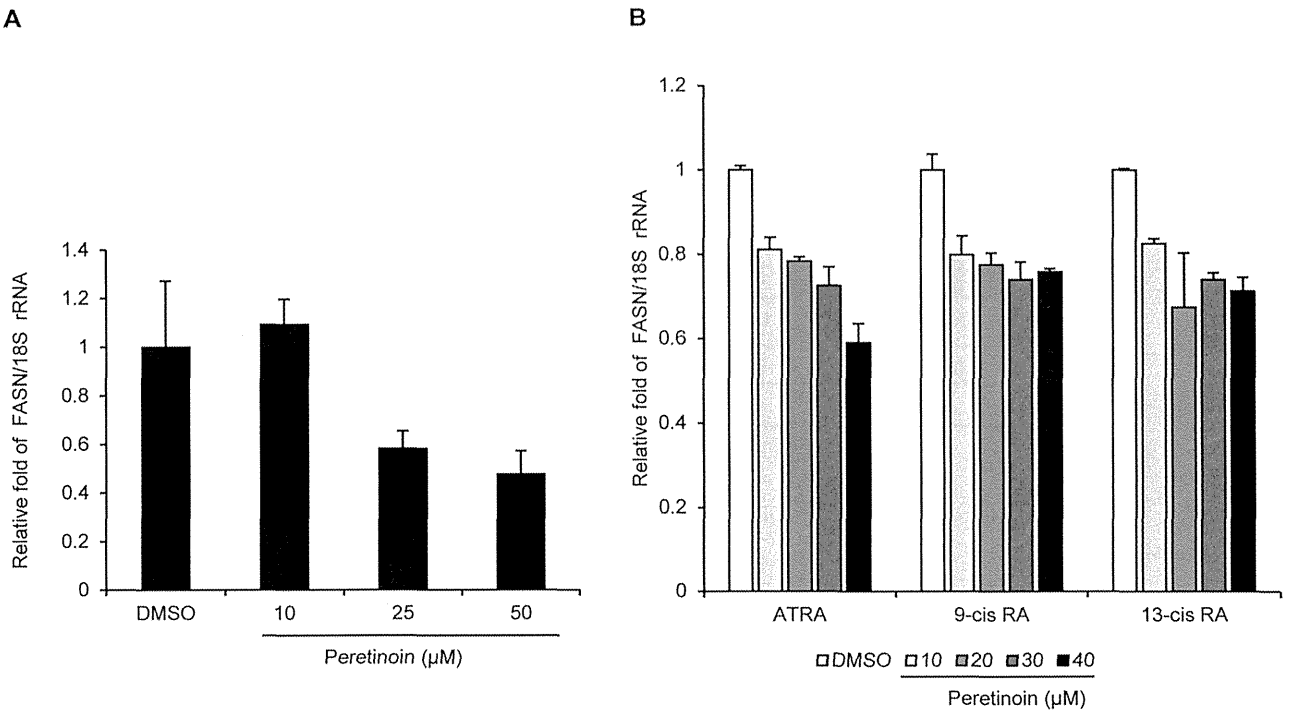

Figure 5 | Reduction of FASN mRNA levels by Peretinoin in a human hepatocyte cell line and the effects of ATRA, 9-cis RA, and 13-cis RA on the expression of FASN mRNA. (A) An immortalised human hepatocyte cell line, THLE-5b cells, was treated with the indicated concentrations of Peretinoin. At 72 h later, RNA was extracted and reverse transcribed, and the levels of FASN mRNA and 18S rRNA were quantified by RTD-PCR. The relative amount of FASN mRNA normalised to that of 18S rRNA is presented as fold change compared to DMSO-treated cells from 3 independent experiments at the indicated conditions. (B) Huh-7.5 cells were transfected with H77S.3/GLuc2A RNA. At 72 h later, the transfected cells were treated with DMSO or 10–40 μM ATRA, 9-cis RA, and 13-cis RA. At 72 h later, RNA was extracted and the levels of FASN mRNA and 18S rRNA were quantified by RTD-PCR. The relative amount of FASN mRNA was determined as described in Fig. 4 and presented as fold change compared to DMSO-treated cells from 3 independent experiments at the indicated conditions.

impaired virus secretion without affecting assembly at 10–30 μM, whilst 40 μM Peretinoin impaired virus secretion and assembly (Fig. 6A). The role of LDs in virus secretion has not been fully characterised, but virus should be secreted through the production and release of very low-density lipoproteins. In addition to microsomal triglyceride transfer protein and several apolipoproteins, such as ApoB and ApoE[23], small interfering RNA screening revealed that multiple components of the secretary pathway, including endoplasmic reticulum to Golgi trafficking and lipid and protein kinases, are involved in HCV secretion[24]. Thus, the mechanism underlying this specific inhibition of virus secretion by Peretinoin remains to be addressed. One possible explanation for its action is the reduction of ApoE3 expression (Fig. 4C), because ApoE3 was shown to have an important role in virus secretion with a minimal impact on assembly[25].

Several reports showed that LDs play an essential role in RNA amplification and virus assembly. The hypolipidemic agent nordihydroguaiaretic acid reduced the number of LDs, resulting in the suppression of RNA amplification and virus secretion, as Peretinoin did[26]. Furthermore, inhibition of tail-interacting protein 47, which coats LDs and is involved in their generation and turnover, suppressed HCV RNA replication and assembly[27,28]. Thus, the inhibition of RNA replication by Peretinoin could be explained by its direct effect on LDs. In addition, a recent report suggested that FASN may localise within HCV replication complexes through an interaction with NS5B, thereby increasing its RNA-dependent RNA polymerase activity[29]. Thus, Peretinoin may inhibit RNA replication not only by reducing the signalling of LDs but also inhibiting the expression of FASN.

We also demonstrated that Peretinoin reduced the levels of mature SREBP1c by inhibiting the proteolysis of its precursor, and subsequently the transcription and expression of FASN (Fig. 4C), which could be the main reason for the alteration of lipid metabolism by Peretinoin; however, the mechanism by which it inhibits proteolysis should be addressed in a future study. Several reports have shown that the expression of SREBP1c and/or FASN is increased in HCV-infected patients[30], Huh-7 cells[31], and a transgenic mouse expressing the full-length HCV polyprotein[32]. In addition, HCV infection was shown to enhance the proteolytic cleavage of precursor SREBP1c, resulting in an increase in its mature form[33]. Taken together, HCV induces lipogenesis to make infected cells more supportive for its propagation. In contrast to HCV, Peretinoin seems to suppress lipogenesis by inhibiting the SREBP1c-FASN axis, which is highly activated by HCV infection. It is also important to note that this effect did not depend on HCV infection, indicating that Peretinoin should exert a hypolipidemic effect, as we also observed a reduction of FASN mRNA levels following Peretinoin treatment of an immortalised human hepatocyte cell line (Fig. 5A). Interestingly, this effect was universal among retinoids because the other retinoids examined also reduced FASN mRNA levels (Fig. 5B). These findings suggest that Peretinoin could also be useful for the treatment of non-alcoholic fatty liver disease, whose hallmark is hepatic fat accumulation.

The antiviral EC_{50} of Peretinoin seems to be closer to its CC_{50} than that of the other retinoids in Huh-7.5 cells because several papers have shown that Peretinoin inhibits the growth of hepatoma cells *in vivo* and *in vitro*[34,35], induces apoptosis in human hepatoma cell lines[36], and causes an arrest of the cell cycle in G0-G1 in human hepatoma cell lines[35], indicating that Peretinoin should selectively

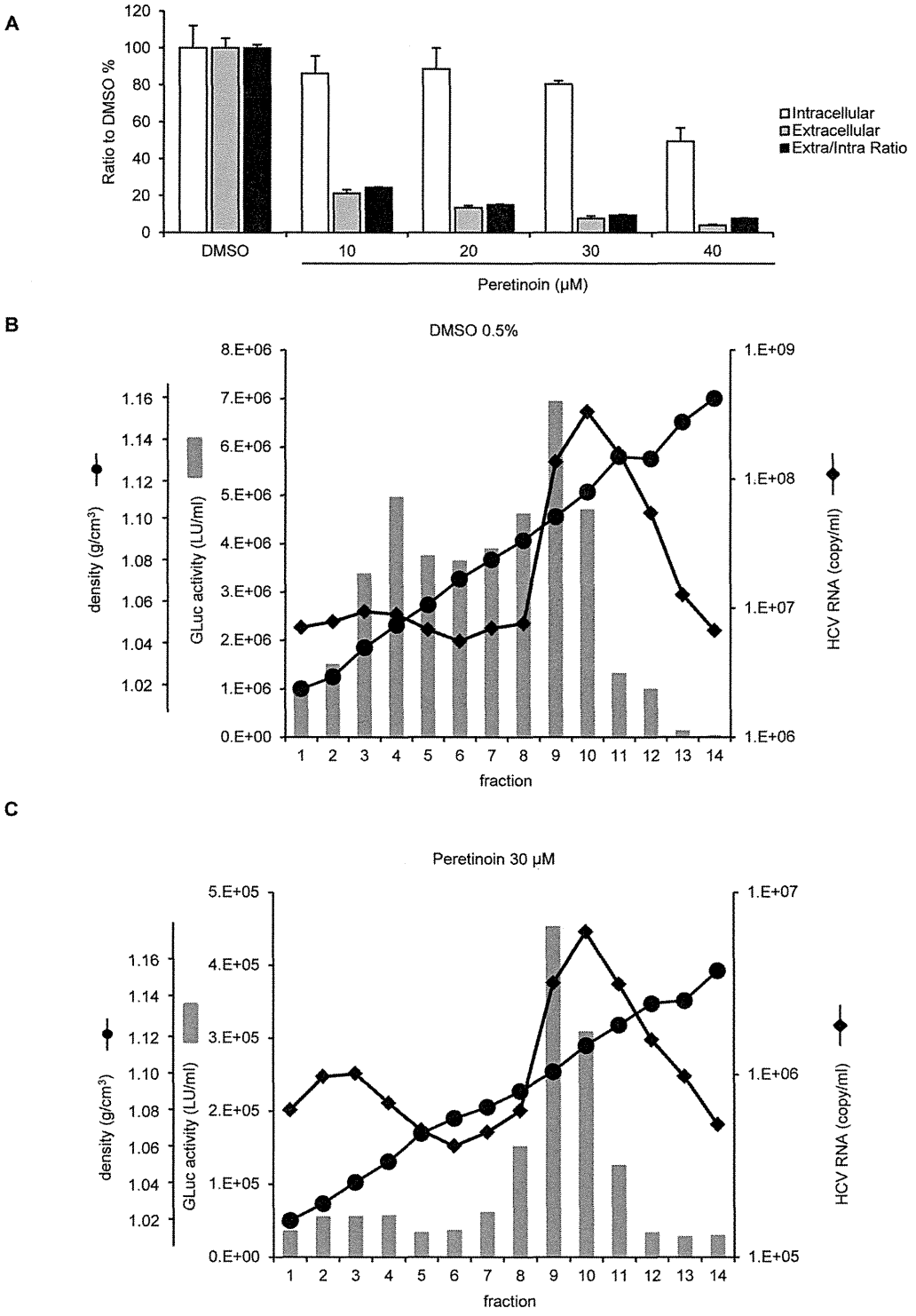

Figure 6 | Impact of Peretinoin on infectious virus production. (A) FT3-7 cells were transfected with HJ3-5/GLuc2A RNA, and 7 days later, 0.5% DMSO, or 10–40 μM Peretinoin, were added. At 72 h later, extra- and intra-cellular viruses were collected and used to infect naïve Huh-7.5 cells. Replication capacity was also determined by measuring secreted GLuc activity. At 48 h after infection, we determined the amount of infectious virus from extra- and intra-cellular media by using GLuc activity as an indicator of the amount of infectious virus. Intra- and extra-cellular infectivity was normalised to replication capacity at infection, and these were then normalised to those of DMSO-treated cells, which were set to 100%. The ratio of extracellular infectious virus to intracellular virus was calculated at the indicated conditions, and it was then normalised to DMSO-treated cells, which were set to 100%. Data show the mean ratio to that of DMSO-treated cells ± SD from 3 independent experiments. (B, C) FT3-7 cells were transfected with HJ3-5/GLuc2A RNA, and 7 days later, 0.5% DMSO or 30 μM Peretinoin were added, and then 72 h later, the medium was collected and subjected to equilibrium ultracentrifugation. Fourteen fractions were taken and analysed for density (circles), HCV RNA levels (diamonds), and infectious virus titres determined by GLuc activity (grey bars). (B) shows the results from DMSO-treated cells, whilst (C) shows those for Peretinoin-treated cells.

suppress the growth of hepatoma cells, although the mechanism has not been fully understood. However, pharmacokinetic data from humans showed that the mean plasma concentration of lipid-bounded Peretinoin is 7.3 μM when patients received 600 mg Peretinoin daily for 8 weeks[37]. This concentration is very close to the antiviral EC_{50} and could have an inhibitory effect on HCV replication, indicating that we could expect an antiviral effect at this dose in humans. Peretinoin showed an additive antiviral effect when combined with IFNα-2b (data not shown); furthermore, HCV did not acquire resistance to Peretinoin after 14 days treatment with 10–40 μM Peretinoin (see Supplementary Fig. S11 online). Although it could be difficult to eradicate HCV only by Peretinoin due to its low selective index (CC50/EC50), combination therapy with Peretinoin plus PEG-IFN, ribavirin, or DAAs may further improve the SVR rate, as vitamin D has been proved to do[38,39].

In summary, we have demonstrated that Peretinoin, which may in the future be administered to patients infected with HCV to prevent HCC, inhibits HCV RNA replication and infectious virus release by modifying several aspects of lipid metabolism.

Methods

Cell lines. Huh-7.5 (kindly provided by Professor C. M. Rice, Rockefeller University, New York, NY), and FT3-7 cells (both clonal derivatives of Huh-7 cells) were maintained as described previously[9]. We used an immortalised human hepatocyte cell line, THLE-5b cells[40], for the indicated experiments.

Reagents. Peretinoin and IFNα-2b were kindly provided by KOWA Company, Ltd. (Tokyo, Japan). ATRA, 9-cis RA, and 13-cis RA, were purchased from Sigma-Aldrich Japan K.K. (Tokyo, Japan). Stock solutions were prepared in DMSO, and all final dilutions contained 0.5% DMSO.

Plasmids. The GLuc coding sequence, followed by the FMDV2A sequence, was inserted between p7 and NS2 in pJFH1 and pHCV-N.2, which encode cDNA of genotype 2a JFH1[13] and genotype 1b N[12], carrying several replication-enhancing mutations to be described elsewhere, respectively, by the same strategy adopted previously for H77S[10]. pH77S.3/GLuc2A[10], pHJ3-5/GLuc2A[9], and pHJ3-5[11] have been described previously.

Antiviral activity assay. The indicated HCV RNAs were transfected by electroporation. The medium was replaced with fresh medium containing serial dilutions of the antiviral compounds at 48 h, and at 24 h intervals thereafter. Secreted GLuc activity was determined at 72 h after adding the antiviral compounds. The concentration of each compound required to reduce the amount of secreted GLuc activity by 50% (EC_{50}) was determined using a 3-parameter Hill equation (Sigma Plot 10.0).

Cell number determination. Huh-7.5 cells were seeded in 96-well plates at a density of 5,000 cells/well, and at 24 h later, the indicated compounds were added. Cell numbers were determined by a WST-8 assay using Cell Counting Kit-8. The concentration of each compound required to reduce the amount of cell number by 50% (CC_{50}) was determined using a 3-parameter Hill equation (Sigma Plot 10.0).

RNA transcription. HCV RNAs were synthesised using a MEGAscript T7 Kit, and synthesised RNA was purified using an RNeasy Mini Kit.

Virus yield determination. Huh-7.5 cells were seeded in 48-well plates at a density of 4.0×10^4 cells/well at 24 h prior to inoculation with 100 μL of virus-containing medium. The cells were maintained at 37°C in a 5% CO_2 environment and fed with 300 μL medium at 24 h later. Following 48 h of additional incubation, the cells were fixed in methanol-acetone (1 : 1) at room temperature for 9 min and stained with a C7-50 monoclonal antibody to the HCV core protein (1 : 300). After extensive washing, the cells were stained with Alexa Fluor 568-conjugated anti-mouse IgG antibodies. A cluster of infected cells staining for core antigen was considered to constitute a single infectious FFU; virus titres are reported as FFUs/mL.

Western blotting and immunostaining. Western blotting and immunostaining were performed as described previously[41,42]. Briefly, the cells were washed in phosphate-buffered saline (PBS) and lysed in a radioimmunoprecipitation assay buffer containing complete Protease Inhibitor Cocktail and PhosSTOP. The membranes were blocked in Blocking One or Blocking One-P solution, and the expression of HCV core protein, FASN, precursor and mature SREBP1c, ApoE3, and β-actin was evaluated with mouse anti-core protein, rabbit anti-FASN, rabbit anti-SREBP1c, goat anti-ApoE3, and rabbit anti-β-actin antibodies, respectively.

For immunofluorescence staining, the cells were washed twice with PBS and fixed in 4% paraformaldehyde for 15 min at room temperature. After washing again with PBS, the cells were permeabilised with 0.05% Triton X-100 in PBS for 15 min at room temperature. They were incubated in a blocking solution (10% foetal bovine serum and 5% bovine serum albumin [BSA] in PBS) for 30 min, and then with the anti-core protein monoclonal antibodies. The fluorescent secondary antibodies were Alexa Fluor 568-conjugated anti-mouse IgG antibodies. Nuclei were labelled with DAPI, and LDs were visualised with BODIPY 493/503. Imaging was performed on a BIOREVO fluorescence microscope (Keyence Corporation, Osaka, Japan). The signal strength of LDs, core protein, and nuclei was quantitated by using Measurement Module BZ-H1M (Keyence Corporation).

Quantitative RTD-PCR. The primer pairs and probes for FASN and 18S rRNA were obtained from the TaqMan assay reagents library. HCV RNA was detected as described previously[43].

Secreted luciferase assay. Cell culture supernatant fluids were collected at intervals after RNA transfection and the cells were re-fed fresh medium. Secreted GLuc was measured as described previously[9].

Fatty acid treatment and measurement of TGs. The cells were treated with the indicated concentrations of OA in the presence of 2% fatty acid-free BSA. Intracellular TG content was measured using a TG Test according to the manufacturer's instructions.

Intra- and extra-cellular infectivity assay. To determine the amount of intra-cellular infectious virus, cell pellets of HJ3-5/GLuc2A-replicating FT3-7 cells harvested after trypsinization were resuspended in complete medium, washed twice with PBS, and lysed by 4 cycles of freezing and thawing. The lysates were clarified by centrifugation at 2,300 × *g* for 5 min prior to inoculation onto naïve Huh-7.5 cells. At the same time, extra-cellular medium was also collected. The medium derived from extra- and intra-cellular cultures was used to infect naïve Huh-7.5 cells, which were plated in 48-well plates at a density of 4.0×10^4 cells/well at 24 h prior to infection. After 6 h inoculation, medium containing virus and possible carryover of Peretinoin was removed by extensive wash, and medium was replaced with fresh one every 24 h until 48 h. At 48 h after infection, we determined GLuc activity and used it as an indicator of the infectious virus titre.

Equilibrium ultracentrifugation of HJ3-5/GLuc2A virus particles using an isopycnic iodixanol gradient. Filtered supernatant fluids collected from HJ3-5/GLuc2A virus-replicating FT3-7 cells treated with DMSO or 30 μM Peretinoin for 72 h were concentrated 30-fold using a Centricon PBHK Centrifugal Plus-20 Filter Unit with an Ultracel-PL membrane (100-kDa exclusion; Merck Millipore, Billerica, MA), then layered on top of a preformed continuous 10–40% iodixanol gradient in Hanks' balanced salt solution. The gradients were centrifuged in an SW41 rotor at 209,678 × *g* for 16 h at 4°C, and fractions (500 μL each) were collected from the top of the tube. The density of each fraction was determined using a digital refractometer. Virus RNA was isolated from each gradient fraction using a QIAamp Viral RNA Kit, and cDNA was synthesised using a High Capacity cDNA Reverse Transcription Kit. RTD-PCR to quantitate the amount of HCV RNA was performed using a 7500 Real Time PCR System. Each fraction was used to infect naïve Huh-7.5 cells for 6 h, followed by extensive washing to ensure GLuc activity was reduced to background. The infected cells were inoculated and the medium was replaced with fresh medium every 24 h. GLuc activity, which was used an alternative to the infectious virus titre, was determined at 72 h after infection.

1. Fried, M. W. *et al.* Peginterferon alfa-2a plus ribavirin for chronic hepatitis C virus infection. *N Engl J Med* **347**, 975–982 (2002).
2. Dabbouseh, N. M. & Jensen, D. M. Future therapies for chronic hepatitis C. *Nat Rev Gastroenterol Hepatol* **10**, 268–276 (2013).
3. Muto, Y. *et al.* Prevention of second primary tumors by an acyclic retinoid, polyprenoic acid, in patients with hepatocellular carcinoma. Hepatoma Prevention Study Group. *N Engl J Med* **334**, 1561–1567 (1996).
4. Muto, Y., Moriwaki, H. & Saito, A. Prevention of second primary tumors by an acyclic retinoid in patients with hepatocellular carcinoma. *N Engl J Med* **340**, 1046–1047 (1999).
5. Okada, H. *et al.* Acyclic retinoid targets platelet-derived growth factor signaling in the prevention of hepatic fibrosis and hepatocellular carcinoma development. *Cancer Res* **72**, 4459–4471 (2012).
6. Shimizu, M. *et al.* Acyclic retinoid inhibits diethylnitrosamine-induced liver tumorigenesis in obese and diabetic C57BLKS/J- +(db)/+Lepr(db) mice. *Cancer Prev Res* **4**, 128–136 (2011).
7. Morbitzer, M. & Herget, T. Expression of gastrointestinal glutathione peroxidase is inversely correlated to the presence of hepatitis C virus subgenomic RNA in human liver cells. *J Biol Chem* **280**, 8831–8841 (2005).
8. Yano, M. *et al.* Comprehensive analysis of the effects of ordinary nutrients on hepatitis C virus RNA replication in cell culture. *Antimicrob Agents Chemother* **51**, 2016–2027 (2007).
9. Shimakami, T. *et al.* Stabilization of hepatitis C virus RNA by an Ago2-miR-122 complex. *Proc Natl Acad Sci U S A* **109**, 941–946 (2012).
10. Shimakami, T. *et al.* Protease inhibitor-resistant hepatitis C virus mutants with reduced fitness from impaired production of infectious virus. *Gastroenterology* **140**, 667–675 (2011).

11. Yi, M., Ma, Y., Yates, J. & Lemon, S. M. Compensatory mutations in E1, p7, NS2, and NS3 enhance yields of cell culture-infectious intergenotypic chimeric hepatitis C virus. *J Virol* **81**, 629–638 (2007).
12. Beard, M. R. *et al.* An infectious molecular clone of a Japanese genotype 1b hepatitis C virus. *Hepatology* **30**, 316–324 (1999).
13. Wakita, T. *et al.* Production of infectious hepatitis C virus in tissue culture from a cloned viral genome. *Nat Med* **11**, 791–796 (2005).
14. Alvisi, G., Madan, V. & Bartenschlager, R. Hepatitis C virus and host cell lipids: an intimate connection. *RNA Biol* **8**, 258–269 (2011).
15. Bassendine, M. F., Sheridan, D. A., Bridge, S. H., Felmlee, D. J. & Neely, R. D. Lipids and HCV. *Semin Immunopathol* **35**, 87–100 (2013).
16. Herker, E. & Ott, M. Emerging role of lipid droplets in host/pathogen interactions. *J Biol Chem* **287**, 2280–2287 (2012).
17. Phan, T., Beran, R. K., Peters, C., Lorenz, I. C. & Lindenbach, B. D. Hepatitis C virus NS2 protein contributes to virus particle assembly via opposing epistatic interactions with the E1–E2 glycoprotein and NS3-NS4A enzyme complexes. *J Virol* **83**, 8379–8395 (2009).
18. Bocher, W. O., Wallasch, C., Hohler, T. & Galle, P. R. All-trans retinoic acid for treatment of chronic hepatitis C. *Liver Int* **28**, 347–354 (2008).
19. Bitetto, D. *et al.* Vitamin A deficiency is associated with hepatitis C virus chronic infection and with unresponsiveness to interferon-based antiviral therapy. *Hepatology* **57**, 925–933 (2013).
20. Hamamoto, S. *et al.* 9-cis retinoic acid enhances the antiviral effect of interferon on hepatitis C virus replication through increased expression of type I interferon receptor. *J Lab Clin Med* **141**, 58–66 (2003).
21. Masaki, T. *et al.* Interaction of hepatitis C virus nonstructural protein 5A with core protein is critical for the production of infectious virus particles. *J Virol* **82**, 7964–7976 (2008).
22. Miyanari, Y. *et al.* The lipid droplet is an important organelle for hepatitis C virus production. *Nat Cell Biol* **9**, 1089–1097 (2007).
23. Shimizu, Y. *et al.* Lipoprotein component associated with hepatitis C virus is essential for virus infectivity. *Curr Opin Virol* **1**, 19–26 (2011).
24. Coller, K. E. *et al.* Molecular determinants and dynamics of hepatitis C virus secretion. *PLoS Pathog* **8**, e1002466 (2012).
25. Hishiki, T. *et al.* Infectivity of hepatitis C virus is influenced by association with apolipoprotein E isoforms. *J Virol* **84**, 12048–12057 (2010).
26. Syed, G. H. & Siddiqui, A. Effects of hypolipidemic agent nordihydroguaiaretic acid on lipid droplets and hepatitis C virus. *Hepatology* **54**, 1936–1946 (2011).
27. Ploen, D. *et al.* TIP47 plays a crucial role in the life cycle of hepatitis C virus. *J Hepatol*, (2013).
28. Vogt, D. A. *et al.* Lipid Droplet-Binding Protein TIP47 Regulates Hepatitis C Virus RNA Replication through Interaction with the Viral NS5A Protein. *PLoS Pathog* **9**, e1003302 (2013).
29. Huang, J. T. *et al.* Hepatitis C Virus Replication Is Modulated by the Interaction of Nonstructural Protein NS5B and Fatty Acid Synthase. *J Virol* **87**, 4994–5004 (2013).
30. Fujino, T. *et al.* Expression profile of lipid metabolism-associated genes in hepatitis C virus-infected human liver. *Hepatol Res* **40**, 923–929 (2010).
31. Yang, W. *et al.* Fatty acid synthase is up-regulated during hepatitis C virus infection and regulates hepatitis C virus entry and production. *Hepatology* **48**, 1396–1403 (2008).
32. Lerat, H. *et al.* Hepatitis C virus proteins induce lipogenesis and defective triglyceride secretion in transgenic mice. *J Biol Chem* **284**, 33466–33474 (2009).
33. Waris, G., Felmlee, D. J., Negro, F. & Siddiqui, A. Hepatitis C virus induces proteolytic cleavage of sterol regulatory element binding proteins and stimulates their phosphorylation via oxidative stress. *J Virol* **81**, 8122–8130 (2007).
34. Muto, Y. & Moriwaki, H. Antitumor activity of vitamin A and its derivatives. *J Natl Cancer Inst* **73**, 1389–1393 (1984).
35. Suzui, M. *et al.* Growth inhibition of human hepatoma cells by acyclic retinoid is associated with induction of p21(CIP1) and inhibition of expression of cyclin D1. *Cancer Res* **62**, 3997–4006 (2002).
36. Nakamura, N. *et al.* Induction of apoptosis by acyclic retinoid in the human hepatoma-derived cell line, HuH-7. *Biochem Biophs Res Commun* **207**, 382–388 (1995).
37. Honda, M. *et al.* Peretinoin, an acyclic retinoid, improves the hepatic gene signature of chronic hepatitis C following curative therapy of hepatocellular carcinoma. *BMC cancer* **13**, 191 (2013).
38. Abu-Mouch, S., Fireman, Z., Jarchovsky, J., Zeina, A. R. & Assy, N. Vitamin D supplementation improves sustained virologic response in chronic hepatitis C (genotype 1)-naive patients. *World J Gastroenterol* **17**, 5184–5190 (2011).
39. Bitetto, D. *et al.* Vitamin D supplementation improves response to antiviral treatment for recurrent hepatitis C. *Transpl Int* **24**, 43–50 (2011).
40. Tokiwa, T. *et al.* Differentiation potential of an immortalized non-tumorigenic human liver epithelial cell line as liver progenitor cells. *Cell Biol Int* **30**, 992–998 (2006).
41. Shirasaki, T. *et al.* La protein required for internal ribosome entry site-directed translation is a potential therapeutic target for hepatitis C virus replication. *J Infect Dis* **202**, 75–85 (2010).
42. Shirasaki, T. *et al.* MicroRNA-27a Regulates Lipid Metabolism and Inhibits Hepatitis C Virus Replication in Human Hepatoma Cells. *J Virol* **87**, 5270–5286 (2013).
43. Honda, M., Shimazaki, T. & Kaneko, S. La protein is a potent regulator of replication of hepatitis C virus in patients with chronic hepatitis C through internal ribosomal entry site-directed translation. *Gastroenterology* **128**, 449–462 (2005).

Acknowledgments

We would like to thank Dr T. Wakita (National Institute of Infectious Disease, Tokyo, Japan) for providing the plasmid encoding JFH1, Dr C. Lee (ThinkSCIENCE INC., Tokyo, Japan) for assistance for medical writing and proof-reading, and Ms Y. Terao (Kanazawa University Hospital, Kanazawa, Japan) for making illustrations. This work was partially supported by the Takeda Science Foundation.

Author contributions

Study design and concept; T.S., T.S. and D.Y., Acquisition of data; T.S., T.S., F.L., K.M., T.S., R.T. and M.F., Drafting of the manuscript; T.S. and T.S., Critical revision of the manuscript for important intellectual content; M.H., D.Y., S.M., S.L. and S.K., Study supervision; M.H. and S.K. All authors reviewed the manuscript.

Additional information

Supplementary information accompanies this paper at http://www.nature.com/scientificreports

Competing financial interests: The authors declare no competing financial interests.

How to cite this article: Shimakami, T. *et al.* The Acyclic Retinoid Peretinoin Inhibits Hepatitis C Virus Replication and Infectious Virus Release *in Vitro*. *Sci. Rep.* **4**, 4688; DOI:10.1038/srep04688 (2014).

HEPATOLOGY
Official Journal of the American Association for the Study of Liver Diseases

Hepatic Interferon-Stimulated Genes Are Differentially Regulated in the Liver of Chronic Hepatitis C Patients With Different Interleukin-28B Genotypes

Masao Honda,[1,2] Takayoshi Shirasaki,[2] Tetsuro Shimakami,[1] Akito Sakai,[1] Rika Horii,[1] Kuniaki Arai,[1] Tatsuya Yamashita,[1] Yoshio Sakai,[1] Taro Yamashita,[1] Hikari Okada,[1] Kazuhisa Murai,[1] Mikiko Nakamura,[2] Eishiro Mizukoshi,[1] and Shuichi Kaneko[1]

Pretreatment up-regulation of hepatic interferon (IFN)-stimulated genes (ISGs) has a stronger association with the treatment-resistant interleukin (IL)28B minor genotype (MI; TG/GG at rs8099917) than with the treatment-sensitive IL28B major genotype (MA; TT at rs8099917). We compared the expression of ISGs in the liver and blood of 146 patients with chronic hepatitis C who received pegylated IFN and ribavirin combination therapy. Gene expression profiles in the liver and blood of 85 patients were analyzed using an Affymetrix GeneChip (Affymetrix, Santa Clara, CA). ISG expression was correlated between the liver and blood of the MA patients, whereas no correlation was observed in the MI patients. This loss of correlation was the result of the impaired infiltration of immune cells into the liver lobules of MI patients, as demonstrated by regional gene expression analysis in liver lobules and portal areas using laser capture microdissection and immunohistochemical staining. Despite having lower levels of immune cells, hepatic ISGs were up-regulated in the liver of MI patients and they were found to be regulated by multiple factors, namely, IL28A/B, IFN-λ4, and wingless-related MMTV integration site 5A (WNT5A). Interestingly, WNT5A induced the expression of ISGs, but also increased hepatitis C virus replication by inducing the expression of the stress granule protein, GTPase-activating protein (SH3 domain)-binding protein 1 (G3BP1), in the Huh-7 cell line. In the liver, the expression of WNT5A and its receptor, frizzled family receptor 5, was significantly correlated with G3BP1. *Conclusions:* Immune cells were lost and induced the expression of other inflammatory mediators, such as WNT5A, in the liver of IL28B minor genotype patients. This might be related to the high level of hepatic ISG expression in these patients and the treatment-resistant phenotype of the IL28B minor genotype. (HEPATOLOGY 2014;59:828-838)

Interferon (IFN) and ribavirin (RBV) combination therapy has been a popular modality for treating patients with chronic hepatitis C (CHC); however, ~50% of patients usually relapse, particularly those with hepatitis C virus (HCV) genotype 1b and a high viral load.[1] The recently developed direct-acting antiviral drug, telaprevir, combined with pegylated (Peg)-IFN plus RBV, significantly improved sustained virologic response (SVR) rates; however, the SVR rate was not satisfactory (29%-33%) in patients who had no

Abbreviations: ALT, alanine aminotransferase; AST, aspartate aminotransferase; CCL, CC chemokine ligand; CHC, chronic hepatitis C; CLLs, cells in liver lobules; CPAs, cells in portal areas; CXCL10/IP-10, chemokine (C-X-C motif) ligand 10/interferon-gamma-induced protein 10; CXCR3, chemokine (C-X-C motif) receptor 3; DCs, dendritic cells; DVL, disheveled; FZD5, frizzled family receptor 5; G3BP1, GTPase-activating protein (SH3 domain)-binding protein 1; GGT, gamma-glutamyl transpeptidase; HCV, hepatitis C virus; IFI44, interferon-induced protein 44; IFIT1, interferon-induced protein with tetratricopeptide repeats 1; IFN, interferon; IHC, immunohistochemical; IL, interleukin; ISGs, interferon-stimulated genes; JFH-1, Japanese fulminant hepatitis type 1; LCM, laser capture microdissection; MA, major genotype; MAd, major genotype, down-regulated; MAu, major genotype, up-regulated; MI, minor genotype; Mx, myxovirus (influenza virus) resistance; NK, natural killer; OAS2, 2′-5′-oligoadenylate synthetase 2; PALT, portal-tract-associated lymphoid tissue; Peg_IFN, pegylated IFN; RBV, ribavirin; RTD-PCR, real-time detection polymerase chain reaction; SG, stress granule; siRNA, small interfering RNA; SVR, sustained virologic response; WNT5A, wingless-related MMTV integration site 5A.

From the [1]Department of Gastroenterology, Kanazawa University Graduate School of Medicine, Kanazawa, Japan; and [2]Department of Advanced Medical Technology, Kanazawa University Graduate School of Health Medicine, Kanazawa, Japan.

Received May 31, 2013; accepted September 30, 2013.

response to previous therapy.[2] Therefore, IFN responsiveness is still an essential clinical determinant for treatment response to triple (Peg-IFN+RBV+DAA) therapy.

A recent landmark genome-wide association study identified a polymorphism in the interleukin (IL)28B, IFN-λ3) gene that was associated with either a sensitive (major genotype; MA) or resistant (minor genotype; MI) treatment response to Peg-IFN and RBV combination therapy and was characterized by either up- (-u) or down-regulation (-d) of interferon-stimulated genes (ISGs).[3-5] However, the underlying mechanism for the association of this polymorphism and treatment response has not been clarified. Previously, we showed that up-regulation of the pretreatment expression of hepatic ISGs was associated with an unfavorable treatment outcome and was closely related to the treatment-resistant IL28B genotype (TG or GG at rs8099917).[6] It could be speculated that the pretreatment activation of ISGs would repress additional induction of ISGs after treatment with exogenous IFN. However, it is unknown how hepatic ISGs are up-regulated in treatment-resistant CHC patients and why patients with high levels of ISG expression cannot eliminate HCV. Therefore, other mechanisms should be involved in the unfavorable treatment outcome of patients with the treatment-resistant IL28B genotype.

In the present study, we performed gene expression profiling in the liver and blood and compared the expression of ISGs between them. Furthermore, ISG expression in liver lobules and portal areas was analyzed separately using a laser capture microdissection (LCM) method. Finally, we identified an immune factor that is up-regulated in patients with the treatment-resistant IL28B genotype and mediates favorable signaling for HCV replication.

Materials and Methods

Patients. We analyzed 168 patients with CHC who had received Peg-IFN-α2b (Schering-Plough K.K., Tokyo, Japan) and RBV combination therapy for 48 weeks at the Graduate School of Medicine, Kanazawa University Hospital, Japan and its related hospitals, as reported previously (Table 1 and Supporting Table 1).[6]

Preparation of Liver Tissue and Blood Samples. A liver biopsy was performed on samples from 168 patients, and blood samples were obtained from 146 of these patients before starting therapy (Table 1 and Supporting Table 1). Detailed procedures are described in the Supporting Materials and Methods.

Affymetrix GeneChip Analysis. Liver tissue samples from 91 patients and blood samples from 85 patients were analyzed using an Affymetrix GeneChip (Affymetrix, Santa Clara, CA). LCM analysis was performed in 5 MAu, MAd, and MI patients. Affymetrix GeneChip analysis and LCM were performed, as described previously.[6,7] Detailed procedures are described in the Supporting Materials and Methods.

Hierarchical Clustering and Pathway Analysis of GeneChip Data. GeneChip data analysis was performed using BRB-Array Tools (http://linus.nci.nih.gov/BRB-ArrayTools.htm), as described previously.[7] Pathway analysis was performed using MetaCore (Thomson Reuters, New York, NY). Detailed procedures are described in the Supporting Materials and Methods.

Quantitative Real-Time Detection Polymerase Chain Reaction, Cell Lines, Cell Migration Assay, Vector Preparation, HCV Replication Analysis, and Statistical Analysis. These procedures are described in detail in the Supplemental Material and Methods.

Results

Differential ISG Expression in Liver and Blood of Patients With Different IL28B Genotypes. Previously, we showed that pretreatment up-regulation of hepatic ISGs was associated with an unfavorable treatment outcome and was closely related to the treatment-resistant IL28B MI (TG or GG at rs8099917).[6] To examine whether expression of hepatic ISGs would reflect the expression of blood ISGs, we compared ISG expression between the liver and blood. We utilized three ISGs (interferon-induced protein 44 [IFI44], interferon-induced protein with

Address reprint requests to: Shuichi Kaneko, M.D., Ph.D., Department of Gastroenterology, Graduate School of Medicine, Kanazawa University, Takara-Machi 13-1, Kanazawa 920-8641, Japan. E-mail: skaneko@m-kanazawa.jp; fax: +81-76-234-4250.

View this article online at wileyonlinelibrary.com.
DOI 10.1002/hep.26788
Potential conflict of interest: Nothing to report.
Additional Supporting Information may be found in the online version of this article.

Table 1. Clinical Characteristics of 146 Patients Whose Liver and Blood Samples Were Analyzed by RT-PCR

	Major (MA)				Minor (MI)		
Clinical Category	Major ISG Up (MAu)		Major ISG Down (MAd)				*P* Value
No. of patients	n = 42		n = 68		n = 36		NA
Age and sex							
Age (years)	55	(30-72)	56	(31-72)	55	(30-73)	NS
Sex (M vs. F)	27 vs. 15		34 vs. 34		19 vs. 17		NS
Treatment responses							
SVR/TR/NR	24/12/6		30/33/6		6/7/23*		MAu vs. MI < 0.0001, MAd vs. MI < 0.0001
IL28B genotype (TT vs. TG+GG)	TT		TT		TG/GG (31/5)		NA
Liver factors							
F stage (1/2/3/4)	14/13/11/4		30/20/11/7		14/8/10/4		NS
A grade (A0-1 vs. A2-3)	16 vs. 26		37 vs. 31		20 vs. 16		NS
ISGs (Mx1, IFI44, IFIT1)	3.83*	(2.14-9.48)	1.30*	(0.36-2.08)	5.52*	(0.86-17.3)	MAu vs. MAd < 0.0001, MAu vs. MI < 0.0001, MAd vs. MI < 0.0001
IL28A/B	41.3*	(4-151)	11.7*	(1-53)	22.7*	(3-93)	MAu vs. MAd < 0.0001, MAu vs. MI = 0.0004, MAd vs. MI = 0.031
Blood factors							
ISGs (Mx1, IFI44, IFIT1)	11.1*	(2.78-24.9)	4.76	(0.41-20.6)	5.64	(0.71-2.8)	MAu vs. MAd < 0.0001, MAu vs. MI < 0.0001
IL28A/B	1.6	(0.1-7.7)	1.3	(0.2-6.4)	1.3	(0.3-3.6)	NS
Laboratory parameters							
HCV-RNA (KIU/mL)	2,430	(160-5,000)	2,692	(140-5,000)	1,854*	(126-5,000)	MAd vs. MI = 0.017
BMI (kg/m2)	24	(18.7-31.9)	24	(16.3-34.7)	22.8	(19.1-30.5)	NS
AST (IU/L)	86*	(22-258)	54	(18-192)	64	(21-178)	MAu vs. MAd = 0.0008
ALT (IU/L)	112*	(17-376)	75	(16-345)	79	(18-236)	MAu vs. MAd = 0.023
γ-GTP (IU/L)	99*	(21-392)	47	(4-367)	74	(20-298)	MAu vs. MAd = 0.0003
WBC (/mm3)	4,761	(2,100-8,100)	4,982	(2,800-9,100)	4,823	(2,500-8,200)	NS
Hb (g/dL)	14.1	(11.4-16.7)	14.1	(9.3-16.9)	13.9	(11.2-16.4)	NS
PLT (× 104/mm3)	15.2	(9.2-27.8)	16.8	(7-39.4)	16.3	(9-27.8)	NS
TG (mg/dL)	112	(42-248)	102	(42-260)	136*	(30-323)	MAd vs. MI = 0.02
T-Chol (mg/dL)	162	(90-221)	169	(107-229)	167	(81-237)	NS
LDL-Chol (mg/dL)	77	(36-123)	83*	(42-134)	72	(29-107)	MAd vs. MI = 0.04
HDL-Chol (mg/dL)	40	(18-67)	43	(27-71)	47*	(27-82)	NS
Viral factors							
ISDR mutations ≦ 1 vs. ≧ 2	23 vs. 19*		51 vs. 17		26 vs. 10		MAu vs. MAd = 0.02
Core aa 70 (wild-type vs. mutant)	24 vs. 18		42 vs. 22		16 vs. 20*		MAd vs. MI = 0.02

*$P < 0.05$.

Abbreviations: BMI, body mass index; ALT, alanine aminotransferase; WBC, leukocytes; Hb, hemoglobin; PLT, platelets; TG, triglycerides; T-chol, total cholesterol; LDL-chol, low density lipoprotein cholesterol; HDL-chol, high density lipoprotein cholesterol; NA, not applicable; NS, not significant.

tetratricopeptide repeats 1 [IFIT1], and myxovirus (influenza virus) resistance [Mx1]) with a high dynamic range, comparable relative expression, and good predictive performance.[6] Mean values of the three ISGs detected by real-time detection polymerase chain reaction (RTD-PCR) in 168 liver tissue samples (Supporting Table 1) showed a significant up-regulation of their expression in nonresponder or treatment-resistant IL28B MI (TG/GG; rs8099917) patients, compared to responder (SVR+TR) or treatment-sensitive IL28B MA (TT; rs8099917) patients, as reported previously (Fig. 1A and Supporting Fig. 1A).[6] However, ISG expression in 146 blood samples (Table 1) showed no difference between responders and nonresponders or the IL28B major and minor genotypes (Fig. 1B and Supporting Fig. 1B). To explore these findings further, gene expression profiling using Affymetrix GeneChips was performed on liver and blood samples from 85 patients (Supporting Tables 2 and 3), and the expression of 37 representative ISGs[6] was compared (Fig. 1C-E). MA patients were divided into two groups according to their ISG expression pattern in the liver: MAu and MAd. MI patients expressed ISGs at a higher level than MAu patients. Interestingly, ISG expression in MA patients showed a similar expression pattern in liver and blood, and ISGs were up-regulated in MAu patients and down-regulated in the MAd patients. However, MI patients showed a different ISG expression pattern in liver and blood, where ISGs were up-regulated in the liver, but down-regulated in the blood (Fig. 1C). The correlation of the mean values of the three ISGs (IFI44, IFIT1, and Mx1) between liver and blood from 146 patients demonstrated a significant correlation between values in MA patients (Fig. 1D), whereas no correlation was observed in MI patients (Fig. 1E). Interestingly, ISG expression correlated significantly between liver and blood of responders, but not of nonresponders, in MA and MI patients (Supporting Fig. 1C-F). These results indicate that the correlation of ISG expression in the liver and blood is an important predictor of treatment response.

Clinical Characteristics of IL28B MA Patients With Up- and Down-Regulated ISGs and IL28B MI Patients. From the expression pattern of ISGs and mean values of the three ISGs (IFI44, IFIT1, and Mx1), we could use receiver operating characteristic curve analysis to set a threshold of 2.1-fold to differentiate MAu and MAd patients. Following this criterion, 42 MAu, 68 MAd, and 36 MI patients (total, 146) were grouped (Table 1). Hepatic ISG expression was highest in MI patients, whereas blood ISG expression was highest in MAu patients. Conversely, hepatic IL28A/B (IFN-λ2/3) expression was highest in MAu patients, whereas blood IL28A/B expression showed no difference among the three groups. Serum alanine aminotransferase (ALT), aspartate aminotransferase (AST), and gamma-glutamyl transpeptidase (GGT) levels were significantly higher in MAu patients than in MAd patients. Interestingly, serum ALT levels were significantly correlated with ISG expression in MA patients, but not in MI patients (Supporting Fig. 2E,F).

Gene expression profiling in peripheral immune cells showed the presence of active inflammation in MAu patients, whereas the inactive or remissive phase of inflammation was observed in MAd patients. In contrast, monophasic and intermediate inflammation existed in MI patients (Supporting Fig. 3).

Reduced Number of Immune Cells in the Liver Lobules of IL28B MI Patients. To examine the discordant expression of ISGs in liver and blood of MI patients, we performed LCM to collect cells in liver lobules (CLLs) and cells in portal areas (CPAs) separately from each of five liver biopsied samples from MAu, MAd, and MI patients (Fig. 2A). Interestingly, the ISG expression pattern in CLLs from MA patients was similar to that of CPAs, and ISGs were up-regulated in MAu patients and down-regulated in MAd patients. ISG expression in CLLs from the MI patients was different to that in CPAs, and ISGs were up-regulated in CLLs, but down-regulated in CPAs (Fig. 2A). We hypothesized that the discordance of ISG expression between CLLs and CPAs in MI patients might be the result of the lower number of immune cells that infiltrated the liver lobules of these patients. To prove this hypothesis, immunohistochemical (IHC) staining was performed (Fig. 2B). IHC staining showed that IFI44 was strongly expressed in the cytoplasm and nucleus of CLLs from MI patients, whereas it was intermediately expressed in MAu patients and weakly expressed in MAd patients. Interestingly, IFI44 was strongly expressed in CPAs of MAu patients and weakly expressed in CPAs of MAd patients, showing a correlation between expression in CLLs and CPAs of MA patients, whereas ILI44 expression was relatively weak in CPAs, compared with CLLs, in MI patients (Fig. 2B). In the same section of the specimens, there were less CD163-positive monocytes and macrophages in MI patients than in MAu and MAd patients. Similarly, there were fewer CD8-positive T cells in MI patients than in MAu and MAd patients (Fig. 2B). Semiquantitative evaluation of CD163- and CD8-positive lymphocytes in liver lobules showed a significantly lower number of cells in

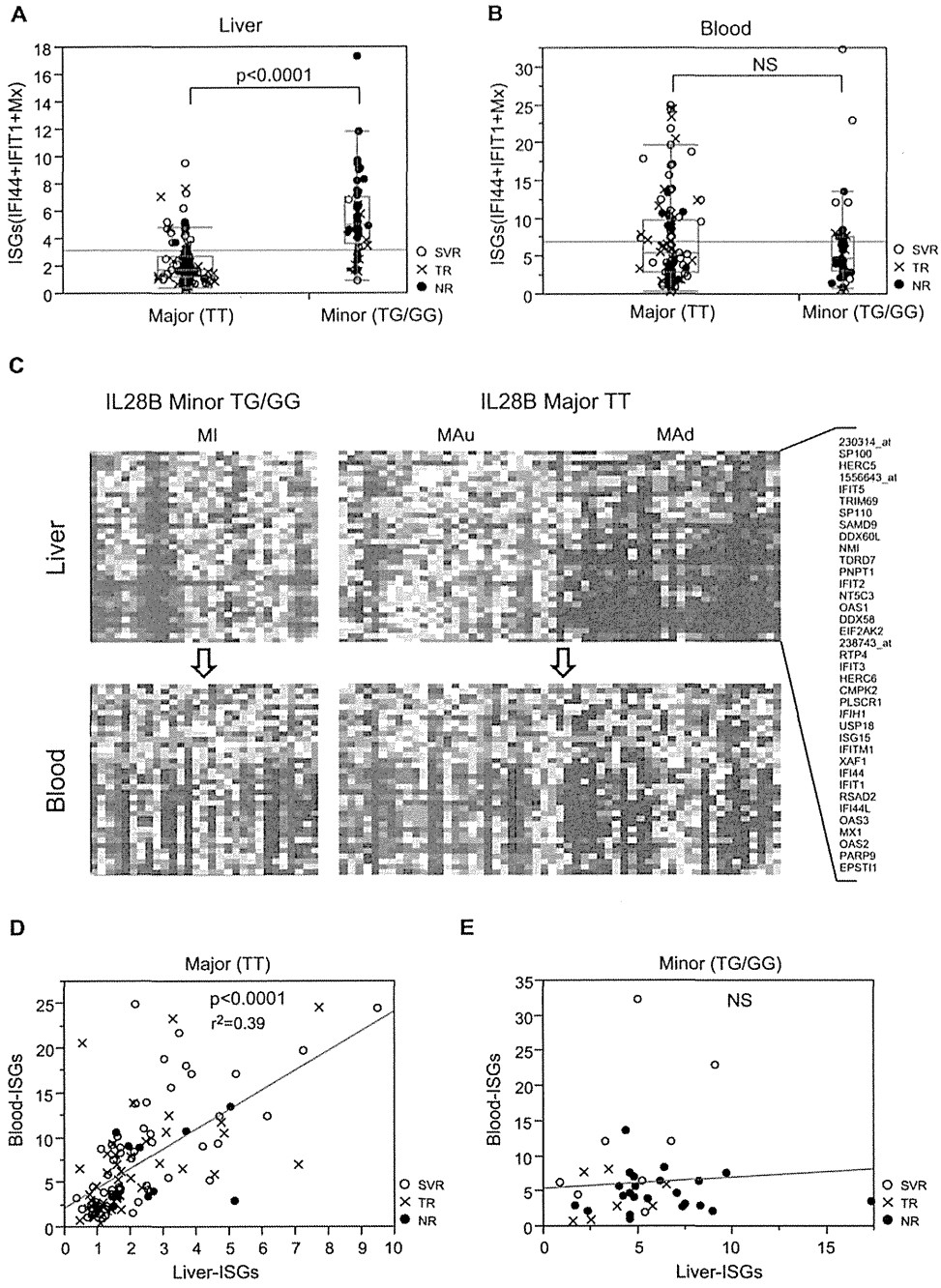

Fig. 1. Comparison of ISG expression in liver and blood of patients with different IL28B genotypes. (A and B) RTD-PCR results of mean ISG expression (IFI44-IFIT1+Mx1) in liver (A) and blood (B) of IL28B major (MAu/Mad) and minor (MI) genotype patients. (C) One-way hierarchical clustering analysis of 85 patients using 37 representative ISGs derived from liver (upper) and blood (lower). (D and E) Correlation of mean ISG expression (IFI44-IFIT1+Mx1) in liver and blood of IL28B major (MA; D) and minor (MI; E) genotype patients.

MI patients than in MAu and MAd patients (Supporting Fig. 4A,B). To support these findings, we examined the expression of 24 surface markers of immune cells in CLL, including dendritic cells (DCs), natural killer (NK) cells, macrophages, T cells, B cells, and granulocytes (Supporting Fig. 5A). The expression of immune cell-surface markers was repressed in MI patients, compared to MAu and MAd patients. Furthermore, whole-liver expression profiling in 85 patients showed the reduced expression of these surface markers in MI patients, compared to MAu and MAd patients (Supporting Fig. 5B). These results indicated that fewer immune cells had infiltrated the liver lobules of MI patients.

In addition to these findings, various chemokines, such as CC chemokine ligand (CCL)19, CCL21, CCL5, and chemokine (C-X-C motif) ligand (CXCL)13, which are important regulators for the recruitment of DCs, NK cells, T cells, and B cells in the liver, were significantly down-regulated in MI patients, compared to MAd and MAu patients (Supporting Fig. 4C-F).

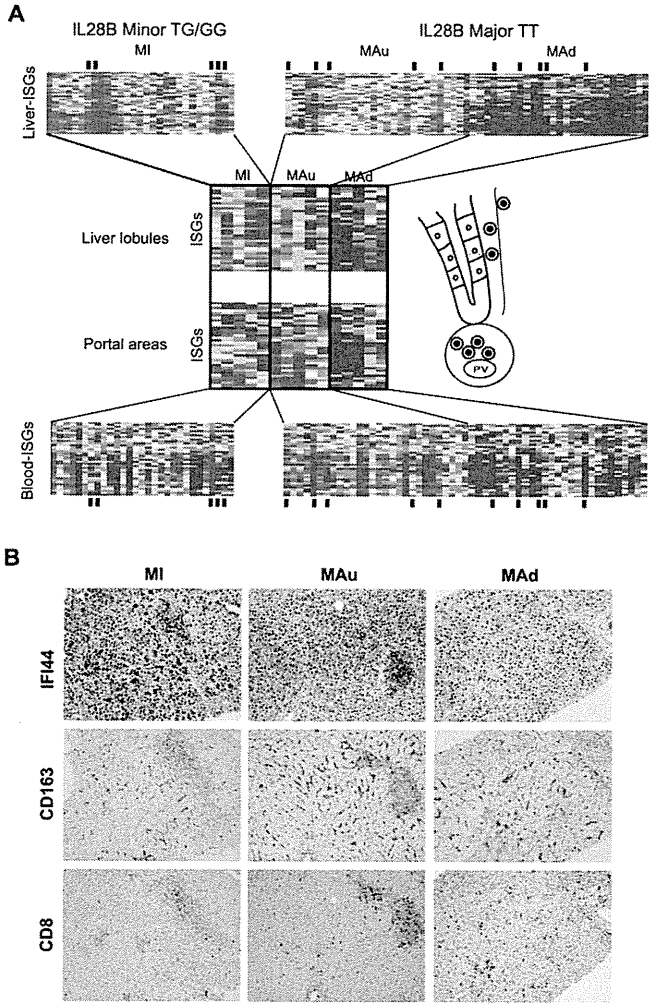

Fig. 2. LCM and IHC staining of biopsied liver specimens. (A) Comparison of the ISG expression pattern of whole liver (upper), CLLs (upper middle), CPAs (lower middle), and blood (bottom). CLLs and CPAs were obtained from 5 MI, MAu, and MAd patients, who are indicated by small black bars. (B) IHC staining of IFI44, CD163, and CD8 in MI, MAu, and MAd patients.

Hepatic ISG Expression Is Significantly Correlated With IL28A/B, but not IFN-α or IFN-β. The lower number of immune cells in the liver lobules of MI patients implies that reduced levels of IFN are produced from DCs, macrophages, and so on. These findings prompted us to examine the relationship between hepatic ISGs and IFN-α, IFN-β, IL29/IFN-λ1, and IL28A/B in CHC patients. Hepatic ISG expression was significantly correlated with IL28A/B, but not IFN-β (Fig. 3A-C) or IFN-α (data not shown) in MAu, MAd, and MI patients. Expression of IL29 was correlated with hepatic ISG expression only in MAu patients. These results indicate that hepatic ISGs would be mainly induced by IL28A/B in CHC patients. Interestingly, the correlation between hepatic ISGs and IL28A/B was strongest in MA patients ($P < 0.0001$ in MAu; $P = 0.0006$ in MAd), whereas rather a weak correlation was observed in MI patients ($P = 0.015$). Moreover, the ratio of hepatic ISGs to IL28A/B was larger in MI patients than in MA patients (S = 0.061 in MI; S = 0.028 in MAu; S = 0.020 in MAd), suggesting the presence of additional factors that can induce expression of ISGs in MI patients. Therefore, we evaluated the expression of the recently discovered IFN-λ4 in MI patients. Interestingly, there was a significant correlation between hepatic ISG and IFN-λ4 expression ($P = 0.0003$; Fig. 3C).

Wingless-Related MMTV Integration Site 5A and Its Receptor, Frizzled Receptor 5, Are Significantly Up-Regulated in the Liver of Patients With the IL28B MI. IFN-λ4 is a promising factor to induce ISG expression in MI patients,[8] and the functional relevance of IFN-λ4 for the pathogenesis of CHC is under investigation. We searched for other factors that could induce ISG expression in MI patients. A closer observation of gene expression profiling in CLLs obtained by LCM demonstrated that WNT signaling was specifically up-regulated in MI patients

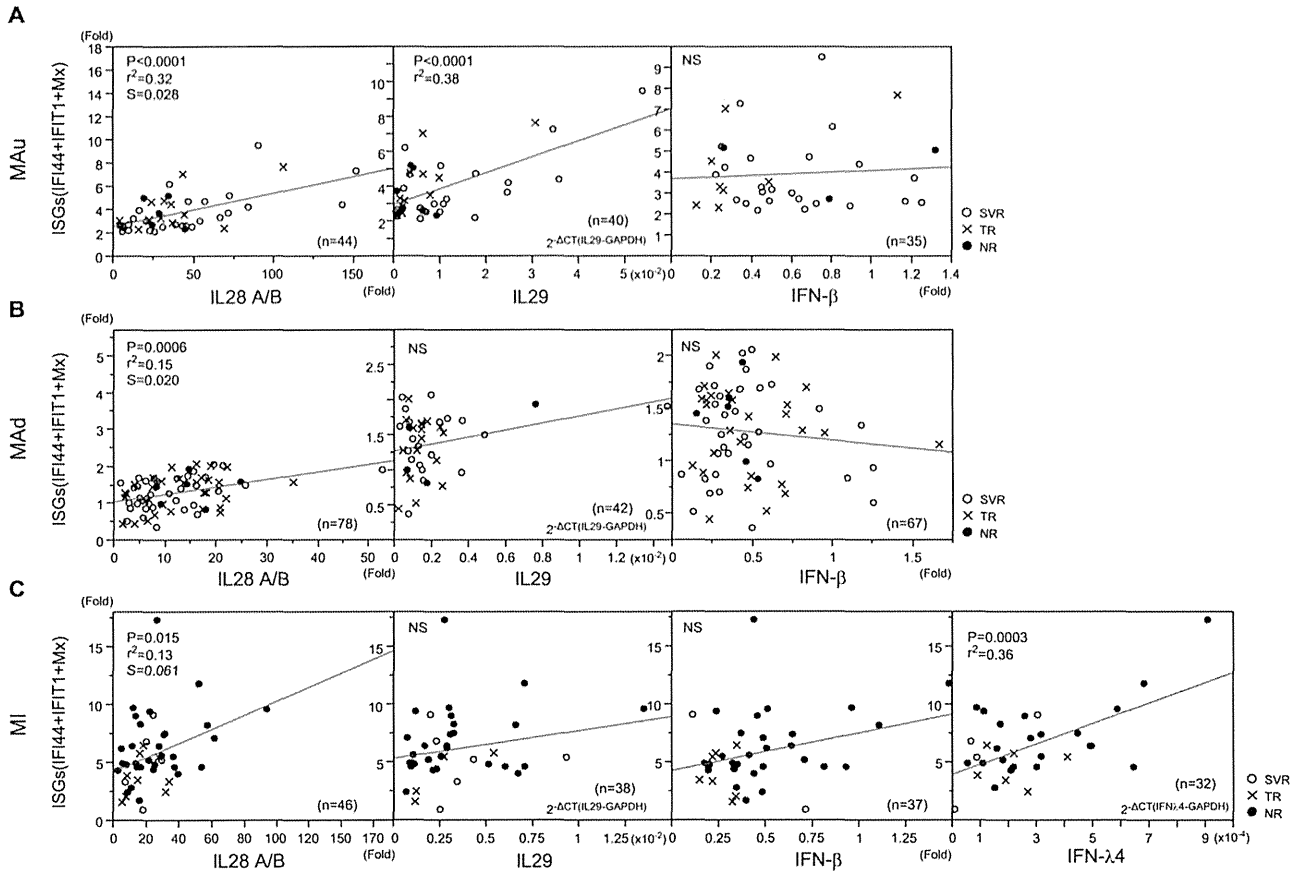

Fig. 3. Correlation analysis of hepatic ISGs and IL28A/B, IL29, IFN-β, and IFN-λ4. Correlation of mean ISG (IFI44+IFIT1+Mx1) and IL28A/B, IL29, IFN-β, and IFN-λ4 expression was evaluated in MAu (A), MAd (B), and MI (C) patients. [Color figure can be viewed in the online issue, which is available at wileyonlinelibrary.com.]

(Supporting Fig. 6). Further observation enabled us to identify that the WNT ligand, wingless-related MMTV integration site 5A (WNT5A), and its receptor, frizzled receptor 5 (FZD5), were up-regulated in MI patients. RTD-PCR results on 168 liver-biopsied samples confirmed the significant up-regulation of WNT5A and FZD5 in MI patients, compared to MAu and MAd patients (Fig. 4A,B). Interestingly, WNT5A expression was negatively correlated with chemokine expression (Supporting Fig. 7). IHC staining showed up-regulation of FZD5 in liver lobules of MI patients, but not in MAu or MAd patients (Fig. 4C). WNT5A expression was significantly correlated with hepatic ISG expression in MI and MAd patients (Fig. 4D). Interestingly, we found a weak, but significant, correlation between WNT5A and IFN-λ4 expression in MI patients (Fig. 4E).

WNT5A Induces ISG Expression, but Stimulates HCV Replication in Huh-7 Cells. To examine the functional relevance of up-regulated expression of WNT5A in MI patients, we first evaluated expression levels of WNT5A and ISGs (2′-5′-oligoadenylate synthetase 2 [OAS2], Mx1, IFI44, and IFIT1) in two immortalized human hepatocyte cell lines, THLE-5b and TTNT cells (Supporting Materials and Methods), and one human hepatoma cell line, Huh-7 cells (Supporting Fig. 8A,B). WNT5A was moderately expressed in THLE-5b and TTNT cells, whereas its expression in Huh-7 cells was minimal. Interestingly, ISG expression in these cells correlated well with expression of WNT5A (Supporting Fig. 8B). Small interfering RNA (siRNA) to WNT5A efficiently repressed WNT5A expression to ~20% of the control in THLE-5b cells, and in this condition, ISG expression was significantly decreased to 30%-50% of the control (Supporting Fig. 8C). Conversely, transduction of WNT5A using a lentivirus expression system in Huh-7 cells significantly increased OAS2 expression (Supporting Fig. 8D), as well as Mx1 and IFIT1 expression (data not shown), in the presence and absence of HCV infection. Surprisingly, HCV replication, as determined using Gaussia luciferase activity, increased in WNT5A-transduced cells (Supporting Fig. 8E). Furthermore, WNT5A-transduced cells supported more HCV replication than

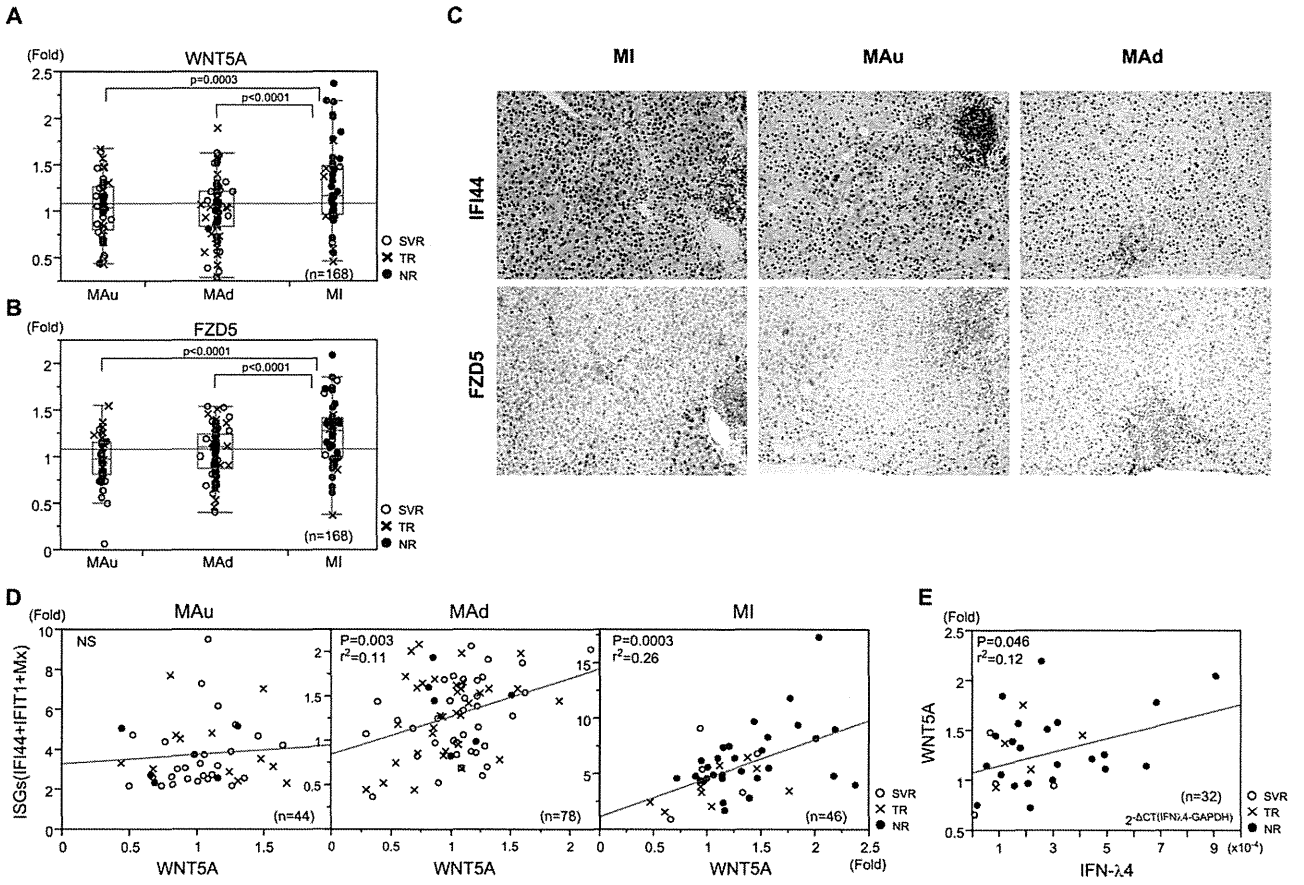

Fig. 4. WNT5A and FZD5 are up-regulated in IL28B MI patients. (A) RTD-PCR results of WNT5A expression in liver of MAu, MAd, and MI patients. (B) RTD-PCR results of FZD5 expression in liver of MAu, MAd, and MI patients. (C) IHC staining of IFI44 and FZD5 expression in liver of MAu, MAd, and MI patients. (D) Correlation of mean ISG (IFI44+IFIT1+Mx1) and WNT5A expression in liver of MAu, MAd, and MI patients. (E) Correlation of WNT5A and IFN-λ4 expression in liver of MI patients.

nontransduced cells under IFN treatment (Supporting Fig. 8F).

WNT5A-FZD5 Signaling Induces the Expression of the Stress Granule Protein, GTPase-Activating Protein (SH3 Domain)-Binding Protein 1, Which Supports HCV Replication. These findings were further confirmed by using Huh-7 cells that were continuously infected with Japanese fulminant hepatitis type 1 (JFH-1; Huh7-JFH1), which is a genotype 2a HCV isolate.[9] Interestingly, expression of WNT5A in Huh7-JFH1 cells was significantly up-regulated, compared with uninfected Huh-7 cells, and showed an equivalent expression level with THLE-5b cells (Fig. 5A). siRNA to WNT5A efficiently repressed WNT5A expression to ~20% of the control, and in this condition, ISG expression (IFI44 was not expressed in Huh-7 cells), HCV RNA, and infectivity were repressed to 25%-65%, 60%, and 40% of the control, respectively (Fig. 5B and Supporting Fig. 9A). Interestingly, CXCL13 expression was significantly increased in this condition. We evaluated the expression of GTPase-activating protein (SH3 domain)-binding protein 1 (G3BP1), a recently recognized stress granule (SG) protein that supports HCV infection and replication.[10] Expression of G3BP1 was repressed to 60% of the control by knocking down WNT5A. Conversely, overexpression of WNT5A in Huh7-JFH1 cells significantly decreased CXCL13 expression and increased HCV RNA, infectivity, and G3BP1 expression (Fig. 5C and Supporting Fig. 9B). A recent report demonstrated that G3BP1 is a disheveled (DVL)-associated protein that regulates WNT signaling downstream of the FZD receptor.[11] Knocking down FZD5 in Huh7-JFH1 cells significantly reduced the expression of DVL1-3, G3BP1, Mx1, and IFIT1 as well as HCV infectivity (Supporting Fig. 9C,D). Interestingly, G3BP1 expression was significantly up-regulated in liver of MI patients (Fig. 5D). Furthermore, G3BP1 expression was significantly correlated with WNT5A expression in liver of the CHC patients (Fig. 5E). More dramatically, a strong correlation was observed between expression of FZD5 and G3BP1 in liver of CHC patients (Fig. 5F).

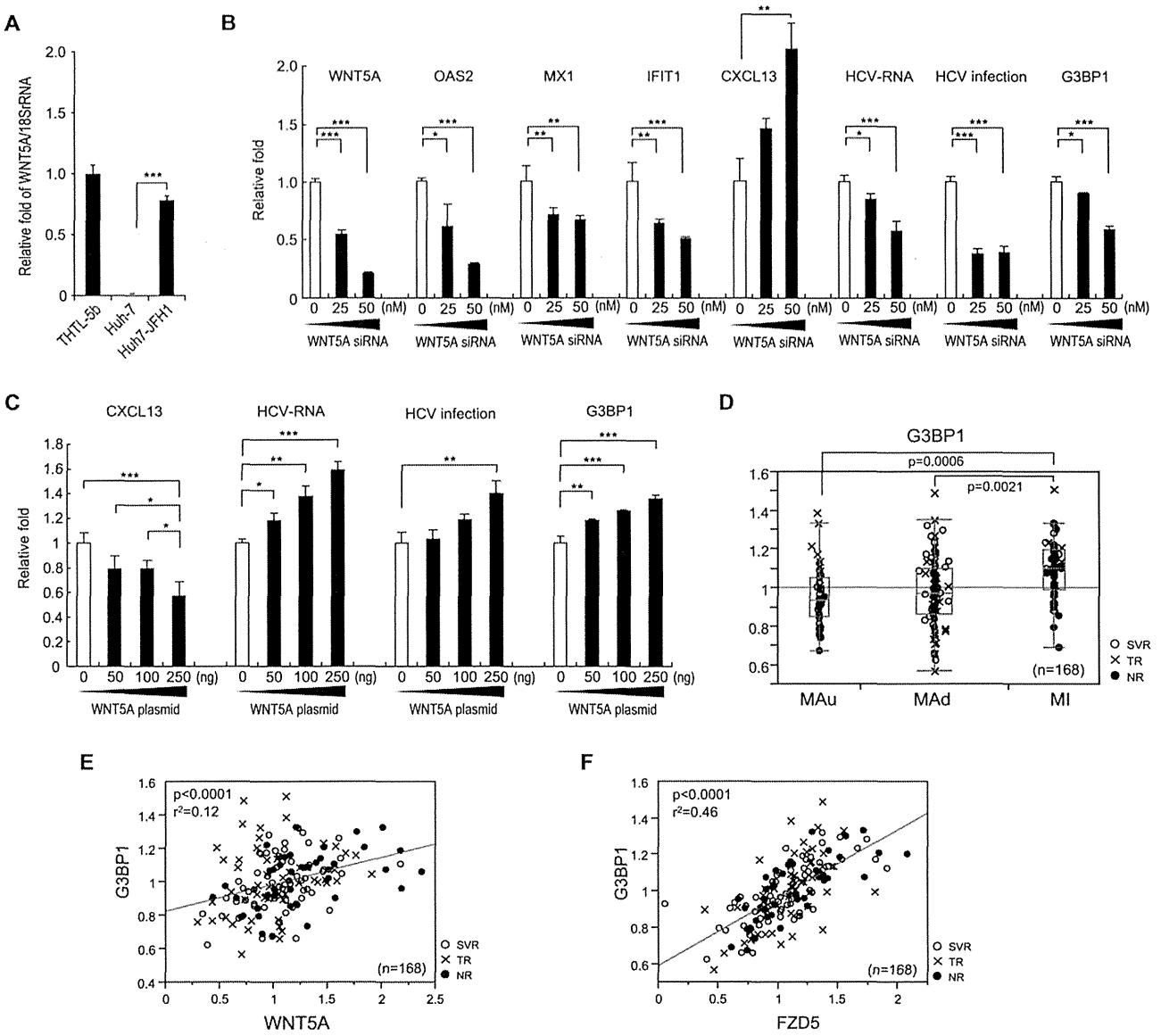

Fig. 5. Relationship between WNT5A and FZD5 signaling and the SG protein, G3BP1. (A) WNT5A expression in THLE-5b, Huh-7, and Huh7-JFH1 cells. (B) Knocking down WNT5A and changes of OAS2, Mx1, IFIT1, CXCL13, and G3BP1 expression, HCV RNA, and infectivity in Huh7-JFH1 cells. (C) Overexpression of WNT5A after transfection with pCMV-WNT5A and decrease in CXCL13 expression and increase in HCV RNA, infectivity, and G3BP1 expression. (A-C) Experiments were performed in duplicate and repeated three times (n = 6). Values are the means ± standard error. $*P < 0.05$; $**P < 0.01$; $***P < 0.005$. (D) RTD-PCR results for G3BP1 expression in liver of MAu, MAd, and MI patients. (E) Correlation of WNT5A and G3BP1 expression in the liver. (F) Correlation of FZD5 and G3BP1 expression in the liver. [Color figure can be viewed in the online issue, which is available at wileyonlinelibrary.com.]

Discussion

The underlying mechanism for the association of the IL28B genotype with treatment responses to IFN-based therapy for HCV has not yet been clarified. We and others have shown that pretreatment up-regulation of hepatic ISGs was associated with an unfavorable treatment outcome[7,12,13] and was closely related to treatment-resistant MI IL28B, compared with treatment-sensitive MA IL28B.[6]

By comparing ISG expression in liver and blood, we found that their expression was correlated in MA patients, but not in MI patients. LCM analysis of ISG expression in CLLs and CPAs showed the loss of the correlation between CLLs and CPAs in MI patients (Fig. 2A). This might be the result of the impaired migration of immune cells into liver lobules that was demonstrated by decreased expression of immune cell-surface markers in CLLs by LCM (Supporting Fig. 5A) and IHC staining (Fig. 2B). Lymphocyte accumulation in the portal area (portal-tract-associated lymphoid tissue; PALT) might be involved in extravasation of lymphocytes from vessels in the portal area, but

others demonstrated that DCs appeared in the sinusoidal wall and passed through the space of Disse to PALT, where the draining lymphatic duct is located.[14] There should be an active movement of immune cells between liver lobules and PALT, as reflected by the correlation of ISG expression in CLLs and CPAs in the MA patients of this study.

ISGs were reportedly up-regulated in hepatocytes of treatment-resistant IL28B genotype patients, but were up-regulated in Kupffer cells of treatment-sensitive genotype patients.[15] Our results confirmed these findings; however, we also showed that expression of various immune cell-surface markers, such as those on DCs, NK cells, macrophages, T cells, B cells, and granulocytes, was lower in MI than in MA patients (Supporting Fig. 5). In addition, we showed that expression of various chemokines was also repressed in MI patients, compared to MA patients (Supporting Fig. 4C-F).

Up-regulation of pretreatment chemokine (C-X-C motif) ligand 10/interferon-gamma-induced protein 10 (CXCL10/IP-10) serum levels is also associated with an unfavorable treatment outcome.[16] CXCL10 expression in the liver was significantly correlated with hepatic ISG expression and was higher in nonresponders than in responders (Supporting Fig. 10). Our results support the usefulness of serum CXCL10 for prediction of treatment outcome. Chemokine (C-X-C motif) receptor 3 (CXCR3) expression, a receptor for CXCL10, was inversely correlated with hepatic ISG expression and was significantly lower in MI than in MA patients (Supporting Fig. 10).

The lower number of immune cells in the liver lobules of MI patients would imply the reduced production of IFN from DCs, macrophages, and so on. Correlation analysis showed that hepatic ISGs were mainly associated with type III IFNs (IL28A/B and IL29), but not type I IFNs (IFN-α or IFN-β), although a significant association with IL29 was only observed in MA patients with up-regulated ISGs. This might be related to the high serum ALT levels in MAu patients (Fig. 3). Closer examination of hepatic ISGs and IL28A/B suggested that factors other than IL28A/B might regulate ISG expression in MI patients. During the preparation of this study, IFN-λ4 was newly identified to be expressed in hepatocytes from treatment-resistant IL28B genotype patients.[8] Interestingly, we found a significant correlation between hepatic ISGs and IFN-λ4 in MI patients (Fig. 3C). Moreover, a closer examination of gene expression profiling in MI patients enabled us to detect up-regulation of the noncanonical WNT ligand, WNT5A. RTD-PCR analysis of 168 patients confirmed up-regulation of WNT5A and its receptor, FZD5, in MI patients. Importantly, WNT5A expression was significantly correlated with hepatic ISG expression in MI patients. A recent report showed that WNT5A induces expression of ISGs, increases sensitivity of keratinocytes to IFN-α,[17] and might be involved in the immune response to influenza virus infection.[18] Therefore, we examined the role of WNT5A in hepatocytes. Interestingly, expression of WNT5A and ISGs was well correlated, and knocking down WNT5A using siRNA reduced expression of ISGs in THLE-5b cells (Supporting Fig. 8). Conversely, transduction of Huh-7 cells with WNT5A using a lentivirus system increased expression of ISGs. Despite the increase in ISG expression, WNT5A did not suppress HCV replication, but rather increased it in Huh-7 cells (Supporting Fig. 8). These results were also confirmed by using Huh-7 cells continuously infected with JFH-1. By knocking down or overexpressing WNT5A in Huh7-JFH1 cells, we showed that HCV-RNA was positively regulated by WNT5A (Fig. 5B,C).

WNT5A and its receptor, FZD5, mediate noncanonical WNT signaling, such as planar cell polarity and the WNT-Ca^{2+}-signaling pathway through G proteins. WNT5A reportedly inhibits B- and T-cell development by counteracting canonical WNT signaling.[19] We found that G3BP1, an SG assembly factor, was up-regulated by WNT5A (Fig. 5C). SGs were reportedly formed by endoplasmic reticulum stress, followed by HCV infection, and localized around lipid droplets with HCV replication complexes.[10] G3BP1 contributes to SG formation and increases HCV replication and infection in Huh-7 cells.[10] Moreover, a recent report demonstrated that G3BP1 is a DVL-associated protein that regulates WNT signaling downstream of the FZD receptor.[11] In this study, repression of WNT5A or FZD5 significantly reduced expression of DVL1-3, G3BP1, Mx1, and IFIT1 as well as HCV infectivity in Huh7-JFH1 cells (Fig. 5 and Supporting Fig. 9).

Importantly, we found a significant correlation between WNT5A and G3BP1 expression in liver tissue samples (Fig. 5E). We also found a significant correlation between FZD5 and G3BP1 expression in liver tissue samples (Fig. 5F). Thus, up-regulated noncanonical WNT5A-FZD5 signaling participates in the induction of ISG expression, but preserves HCV replication and infection in hepatocytes by increasing levels of the SG protein, G3BP1. These findings may explain the pathophysiological state of the treatment-resistant phenotype in MI patients.

In this study, we demonstrated impaired immune cell infiltration of the liver in treatment-resistant IL28B genotype patients, and we also demonstrated

that up-regulation of hepatic ISGs in treatment-resistant IL28B genotype patients was mediated by multiple factors, including IL28A/B, IFN-λ4, and WNT5A. We found a significant negative correlation between WNT5A and various chemokines in liver of CHC patients (Supporting Fig. 7). Interestingly, WNT5A directly repressed one of these chemokines, CXCL13, a B-lymphocyte chemoattractant, in HCV-infected hepatocytes. These results indicate that loss of immune cells from the liver may be associated with the induction of other inflammatory factors, such as WNT5A, in MI patients, although we did not identify which cells express WNT5A. Further studies are needed to explore their functional relevance in the pathogenesis of CHC.

Acknowledgment: The authors thank Mina Nishiyama for her technical assistance.

References

1. Fried MW, Shiffman ML, Reddy KR, Smith C, Marinos G, Goncales FL, Jr., et al. Peginterferon alfa-2a plus ribavirin for chronic hepatitis C virus infection. N Engl J Med 2002;347:975-982.
2. Zeuzem S, Andreone P, Pol S, Lawitz E, Diago M, Roberts S, et al. Telaprevir for retreatment of HCV infection. N Engl J Med 2011;364:2417-2428.
3. Ge D, Fellay J, Thompson AJ, Simon JS, Shianna KV, Urban TJ, et al. Genetic variation in IL28B predicts hepatitis C treatment-induced viral clearance. Nature 2009;461:399-401.
4. Suppiah V, Moldovan M, Ahlenstiel G, Berg T, Weltman M, Abate ML, et al. IL28B is associated with response to chronic hepatitis C interferon-alpha and ribavirin therapy. Nat Genet 2009;41:1100-1104.
5. Tanaka Y, Nishida N, Sugiyama M, Kurosaki M, Matsuura K, Sakamoto N, et al. Genome-wide association of IL28B with response to pegylated interferon-alpha and ribavirin therapy for chronic hepatitis C. Nat Genet 2009;41:1105-1109.
6. Honda M, Sakai A, Yamashita T, Nakamoto Y, Mizukoshi E, Sakai Y, et al. Hepatic ISG expression is associated with genetic variation in interleukin 28B and the outcome of IFN therapy for chronic hepatitis C. Gastroenterology 2010;139:499-509.
7. Honda M, Nakamura M, Tateno M, Sakai A, Shimakami T, Shirasaki T, et al. Differential interferon signaling in liver lobule and portal area cells under treatment for chronic hepatitis C. J Hepatol 2010;53:817-826.
8. Prokunina-Olsson L, Muchmore B, Tang W, Pfeiffer RM, Park H, Dickensheets H, et al. A variant upstream of IFNL3 (IL28B) creating a new interferon gene IFNL4 is associated with impaired clearance of hepatitis C virus. Nat Genet 2013;45:164-171.
9. Wakita T, Pietschmann T, Kato T, Date T, Miyamoto M, Zhao Z, et al. Production of infectious hepatitis C virus in tissue culture from a cloned viral genome. Nat Med 2005;11:791-796.
10. Garaigorta U, Heim MH, Boyd B, Wieland S, Chisari FV. Hepatitis C virus (HCV) induces formation of stress granules whose proteins regulate HCV RNA replication and virus assembly and egress. J Virol 2012;86:11043-11056.
11. Bikkavilli RK, Malbon CC. Arginine methylation of G3BP1 in response to Wnt3a regulates beta-catenin mRNA. J Cell Sci 2011;124:2310-2320.
12. Sarasin-Filipowicz M, Oakeley EJ, Duong FH, Christen V, Terracciano L, Filipowicz W, Heim MH. Interferon signaling and treatment outcome in chronic hepatitis C. Proc Natl Acad Sci U S A 2008;105:7034-7039.
13. Chen L, Borozan I, Feld J, Sun J, Tannis LL, Coltescu C, et al. Hepatic gene expression discriminates responders and nonresponders in treatment of chronic hepatitis C viral infection. Gastroenterology 2005;128:1437-1444.
14. Kudo S, Matsuno K, Ezaki T, Ogawa M. A novel migration pathway for rat dendritic cells from the blood: hepatic sinusoids-lymph translocation. J Exp Med 1997;185:777-784.
15. Chen L, Borozan I, Sun J, Guindi M, Fischer S, Feld J, et al. Cell-type specific gene expression signature in liver underlies response to interferon therapy in chronic hepatitis C infection. Gastroenterology 2010;138:1123-1133.e1-3.
16. Askarieh G, Alsio A, Pugnale P, Negro F, Ferrari C, Neumann AU, et al. Systemic and intrahepatic interferon-gamma-inducible protein 10 kDa predicts the first-phase decline in hepatitis C virus RNA and overall viral response to therapy in chronic hepatitis C. HEPATOLOGY 2010;51:1523-1530.
17. Romanowska M, Evans A, Kellock D, Bray SE, McLean K, Donandt S, Foerster J. Wnt5a exhibits layer-specific expression in adult skin, is upregulated in psoriasis, and synergizes with type 1 interferon. PLoS One 2009;4:e5354.
18. Shapira SD, Gat-Viks I, Shum BO, Dricot A, de Grace MM, Wu L, et al. A physical and regulatory map of host-influenza interactions reveals pathways in H1N1 infection. Cell 2009;139:1255-1267.
19. Staal FJ, Luis TC, Tiemessen MM. WNT signalling in the immune system: WNT is spreading its wings. Nat Rev Immunol 2008;8:581-593.

THE JOURNAL OF BIOLOGICAL CHEMISTRY VOL. 289, NO. 1, pp. 335–345, January 3, 2014

Metformin Suppresses Expression of the Selenoprotein P Gene via an AMP-activated Kinase (AMPK)/FoxO3a Pathway in H4IIEC3 Hepatocytes*[S]

Received for publication, May 1, 2013, and in revised form, November 18, 2013 Published, JBC Papers in Press, November 20, 2013, DOI 10.1074/jbc.M113.479386

Hiroaki Takayama,[a] Hirofumi Misu,[a] Hisakazu Iwama,[b] Keita Chikamoto,[a,c] Yoshiro Saito,[d] Koji Murao,[e] Atsushi Teraguchi,[f] Fei Lan,[a] Akihiro Kikuchi,[a] Reina Saito,[a] Natsumi Tajima,[a] Takayoshi Shirasaki,[a,g] Seiichi Matsugo,[h,i] Ken-ichi Miyamoto,[j,k] Shuichi Kaneko,[a] and Toshinari Takamura[a1]

From the [a]Department of Disease Control and Homeostasis, Kanazawa University Graduate School of Medical Sciences, 13-1 Takara-machi, Kanazawa, Ishikawa 920-8641, Japan, the [b]Life Science Research Center, Kagawa University, Ikenobe 1750-1, Miki-cho, Kita-gun, Kagawa 761-0793, Japan, the [c]Division of Natural System, Graduate School of Natural Science and Technology, Kanazawa University, Kakuma-machi, Kanazawa, Ishikawa 920-1192, Japan, the [d]Systems Life Sciences, Department of Medical Life Systems, Faculty of Medical and Life Sciences, Doshisha University, Kyotanabe, Kyoto 610-0394, Japan, the [e]Departments of Advanced Medicine, Kagawa University, Ikenobe 1750-1, Miki-cho, Kita-gun, Kagawa 761-0793, Japan, the [f]Department of Hospital Pharmacy, Kanazawa University, 13-1 Takara-machi, Kanazawa, Ishikawa 920-8641, Japan, the [g]Department of Advanced Medical Technology, Kanazawa University Graduate School of Health Medicine, 13-1 Takara-machi, Kanazawa, Ishikawa 920-8641, Japan, the [h]Division of Material Engineering, Graduate School of Natural Science and Technology, Kanazawa University, Kakuma-machi, Kanazawa, Ishikawa 920-1192, Japan, the [i]Institute of Science and Engineering, Faculty of Natural System, Kanazawa University, Kakuma-machi, Kanazawa, Ishikawa 920-1192, Japan, the [j]Department of Hospital Pharmacy, Kanazawa University Graduate School of Medical Sciences, 13-1 Takara-machi, Kanazawa, Ishikawa 920-8641, Japan, and the [k]Department of Medicinal Informatics, Kanazawa University Graduate School of Medical Sciences, 13-1 Takara-machi, Kanazawa, Ishikawa 920-8641, Japan

Background: The suppression of selenoprotein P production may be a novel therapeutic target for reducing insulin resistance.
Results: Selenoprotein P expression was suppressed by metformin treatment, but co-administration of AMPK inhibitor or FoxO3a siRNA cancelled this suppression.
Conclusion: Metformin suppresses selenoprotein P expression via the AMPK/FoxO3a pathway.
Significance: The AMPK/FoxO3a pathway in the liver may be a therapeutic target for type 2 diabetes.

Selenoprotein P (SeP; encoded by *SEPP1* in humans) is a liver-derived secretory protein that induces insulin resistance in type 2 diabetes. Suppression of SeP might provide a novel therapeutic approach to treating type 2 diabetes, but few drugs that inhibit *SEPP1* expression in hepatocytes have been identified to date. The present findings demonstrate that metformin suppresses *SEPP1* expression by activating AMP-activated kinase (AMPK) and subsequently inactivating FoxO3a in H4IIEC3 hepatocytes. Treatment with metformin reduced *SEPP1* promoter activity in a concentration- and time-dependent manner; this effect was cancelled by co-administration of an AMPK inhibitor. Metformin also suppressed *Sepp1* gene expression in the liver of mice. Computational analysis of transcription factor binding sites conserved among the species resulted in identification of the FoxO-binding site in the metformin-response element of the *SEPP1* promoter. A luciferase reporter assay showed that metformin suppresses Forkhead-response element activity, and a ChIP assay revealed that metformin decreases binding of FoxO3a, a direct target of AMPK, to the *SEPP1* promoter. Transfection with siRNAs for *Foxo3a*, but not for *Foxo1*, cancelled metformin-induced luciferase activity suppression of the metformin-response element of the *SEPP1* promoter. The overexpression of FoxO3a stimulated *SEPP1* promoter activity and rescued the suppressive effect of metformin. Metformin did not affect FoxO3a expression, but it increased its phosphorylation and decreased its nuclear localization. These data provide a novel mechanism of action for metformin involving improvement of systemic insulin sensitivity through the regulation of SeP production and suggest an additional approach to the development of anti-diabetic drugs.

Selenoprotein P (SeP[2]; encoded by *SEPP1* in humans) is a secretory protein produced mainly by the liver (1, 2). SeP contains 10 selenocysteine residues and is known to transport the essential trace element selenium from the liver to the rest of the

* This work was supported by grants-in-aid from the Ministry of Education, Culture, Sports, Science and Technology, Japan (to H. M., T. T., and S. K.) and research grants from Dainippon Sumitomo Pharma (to S. K.) and Takeda Science Foundation (to H. M.).
[S] This article contains supplemental Figs. S1–S5.
[1] To whom correspondence should be addressed: Dept. of Disease Control and Homeostasis, Kanazawa University Graduate School of Medical Science, 13-1 Takara-machi, Kanazawa, Ishikawa 920-8641, Japan. Tel.: 81-76-265-2233; Fax: 81-76-234-4250; E-mail: ttakamura@m-kanazawa.jp.

[2] The abbreviations used are: SeP, selenoprotein P; AMPK, AMP-activated kinase; AICAR, 5-aminoimidazole-4-carboxamide ribonucleotide; compound C, 6-[4-(2-piperidin-1-yl-ethoxy)-phenyl)]-3-pyridin-4-yl-pyrrazolo[1,5-a]-pyrimidine; cGPx, cellular glutathione peroxidase; DN, dominant negative; CA, constitutive active; TFBS, transcription factor binding site; FHRE, forkhead-response element.